applied sciences

MDPI

Review

Review of Functionally Graded Thermal Sprayed Coatings

Leszek Łatka [1,*], Lech Pawłowski [2,*], Marcin Winnicki [1], Pawel Sokołowski [1], Aleksandra Małachowska [1] and Stefan Kozerski [1]

[1] Faculty of Mechanical Engineering, Wrocław University of Science and Technology, 5 Łukasiewicza Street, 50-371 Wrocław, Poland; marcin.winnicki@pwr.edu.pl (M.W.); pawel.sokolowski@pwr.edu.pl (P.S.); aleksandra.malachowska@pwr.edu.pl (A.M.); stefan.kozerski@pwr.edu.pl (S.K.)

[2] IRCER, UMR CNRS 7315, Department of Physics, Faculty of Sciences and Technology, University of Limoges, 12, rue Atlantis, 87068 Limoges, France

* Correspondence: leszek.latka@pwr.edu.pl (L.Ł.); lech.pawlowski@unilim.fr (L.P.)

Received: 1 July 2020; Accepted: 20 July 2020; Published: 27 July 2020

Abstract: The paper briefly describes major thermal spray techniques used to spray functionally graded coatings such as atmospheric plasma spraying, high velocity oxy-fuel spraying, suspension and solution precursor plasma spraying, and finally low and high pressure cold gas spray method. The examples of combined spray processes as well as some examples of post spray treatment including laser and high temperature treatments or mechanical one, are described. Then, the solid and liquid feedstocks used to spray and their properties are shortly discussed. The reviewed properties of functional coatings include: (i) mechanical (adhesion, toughness, hardness); (ii) physical (porosity, thermal conductivity and diffusivity, thermal expansion, photo-catalytic activity), and; (iii) bioactivity and simulated body fluid (SBF) corrosion. These properties are useful in present applications of functionally graded coatings as thermal barriers, the bioactive coatings in prostheses, photo-catalytic coatings in water treatment, coatings used in printing industry (anilox and corona rolls). Finally, some of the future possible fields of functional thermal sprayed coatings applications are discussed, e.g., to coat polymer substrates or to use the cheap technology of low pressure cold gas spray method instead of expensive technology of vacuum plasma spraying to obtain bond coatings.

Keywords: thermal spray coatings; functional graded coatings; application of thermal spray coatings

1. Introduction

Thermally sprayed coatings can be obtained using a number of methods enabling different type of materials such as metals and their alloys and ceramics (mainly oxides and carbides) to be deposited. Also the composites of metal and alloys with ceramics are also very frequently sprayed [1]. Another group of materials, namely the polymer is also possible to spray and the deposits of thermoplastic polymers as polymethylmetacrylate and fluoropolymers are described in the literature [2,3].

The coatings can be applied to protect the substrates of all type of materials. Metals and alloys are used as substrates very frequently. However, ceramics or polymer substrates are also used. That is why there are many new industrial applications of coatings. The entire thermal spraying (TS) market was estimated in the beginning of XXI century to be 2 billion € [1] and it grew up in 2018 up to 7.4 billion US$ (i.e., about 6.6 billion €) and the projection for 2026 is 13.5 billion US$ (12 billion €) [4].

The main function of coatings is to protect the substrates of all types of harmful agents. The latter may act destructively starting from coatings surface in the following ways, such as e.g.,:

- Mechanical, by action of abrasion, erosion, or friction of external bodies;
- Physical, and in particular, thermophysical, by submitting the substrate to high temperature and to intensive heat flux;
- Chemical or biochemical, by reaction of external compounds with substrate.

The protection of substrate is realized by the coatings that belong, generally, to another group of materials than substrate. For example, ceramics protect metals and alloys against wet corrosion or high temperature. Knowing that many properties of such coating are very different from that of substrate, their direct application may lead to generation of mechanical or thermal stresses at their interface. A reasonable way leading to reduce them is the design of multi-coatings with the gradient of composition. The design of multi-coatings requires that the coating being in contact with substrate should be reasonably similar to substrate properties. Inversely, the one being in contact with outer environment has to have the properties enabling to fulfill the protective function of the deposit. This is a fundamental concept of functionally graded coatings presented in this paper.

An important issue in the design of functionally graded coatings is the prediction in which properties are essential to fulfill the functions in service. That is why the properties of the coatings are shortly described. The properties depend strongly on the coatings' microstructure resulting from the method of thermal spraying, and in particular, on the feedstock used to spray. Some of the methods as well as solid (powders) and liquid feedstock (solution and suspension) are shortly described.

Finally, some practical applications of functionally graded coatings are shown and the perspective of their future development are briefly depicted.

2. Spray Techniques and Feedstock Used to Deposit Functionally Graded Coatings

This chapter describes briefly the thermal spray methods used frequently to obtain functionally graded coatings i.e., plasma spraying with solid and liquid feedstock, high velocity oxy fuel spraying and cold spraying. Moreover, the feedstock used to spray and the post-spray treatments methods are shown.

2.1. Atmospheric Plasma Spraying (APS)

There are many methods of coatings manufacturing on the field of TS. Among them, plasma spraying is one of the most frequently used, because of very wide range of applications and of reasonable cost of equipment [1]. The basic technique is atmospheric plasma spraying (APS). First patents, associated to the introduction of the method in the industry, were attributed in the beginning of 1960s [5,6]. The careful description of this method is made in [1,7].

The sketch of the APS method is shown in Figure 1 (inspired by [8]). The electrical arc is ignited between copper anode and thoriated tungsten cathode. Plasma gases are ionized, heated, and expanded forming the plasma jet. Then, the powder particles, being transported by a carrier gas, are injected to the hot stream of plasma jet, which are submitted to heating and to acceleration by drag force. Then, these particles hit into the substrate with relatively high kinetic energy and form splats. Finally, the splats solidify and build up the coating [1,7].

The fundamental process parameter is the composition of working gas composition. Two main groups of gases are used: (i) primary; and (ii) secondary ones. The primary gas is frequently argon (Ar) and sometimes nitrogen (N_2). The primary gas should stabilize arc inside the torch's nozzle. The secondary gases is added to increase heat conductivity of plasma [1,9].

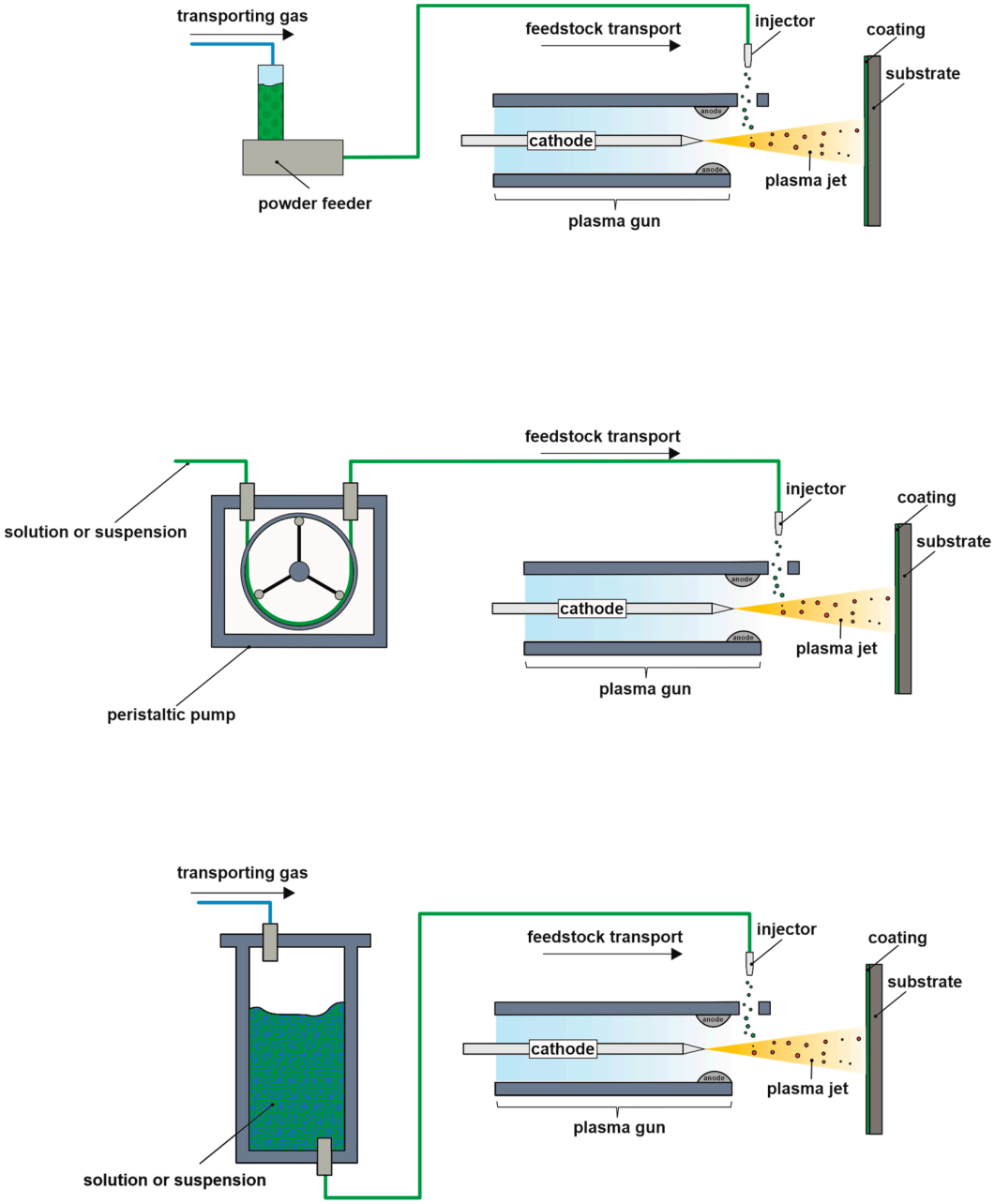

Figure 1. Schematic representation of the plasma spray deposition processes: atmospheric plasma spraying (APS) (up) and suspension plasma spraying (SPS) and solution precursor plasma spraying (SPPS)—(down) inspired by [8].

Other important APS parameters are as follows [10]:

- Electrical power;
- Flow rate of the plasma gases;
- Feed-rate of used powder and its size distribution (most frequently, the particles sizes are in the range from 20 up to 90 microns);
- Relative speed velocity of plasma torch with regards to the substrate [10].

Nevertheless, there are many other parameters, which influence also the coatings structure and properties. Therefore, their optimization is very important [11–13].

The microstructure of sprayed coatings results from the phenomena occurring inside the powder particle in plasma jet (see Figure 2). The appropriate choice of spray parameters should lead to melting

of injected particles before their impact on the substrate. However, the powders include frequently small and large particles. The small powder's particles may get molten in plasma and start to evaporate. On the other hand, the large ones may remain solid.

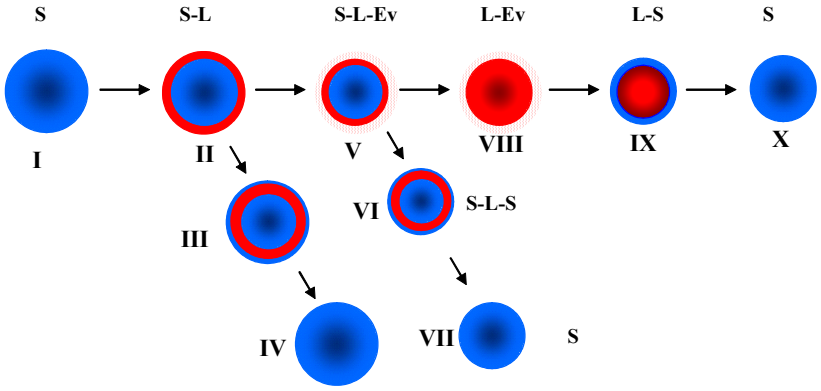

Figure 2. The phenomena occurring after injection of solid powder particle in plasma jet at APS [14]. The symbols described the phases in a particle: S, solid; L, liquid; and Ev, evaporated gas. Reproduced with permission from [Wiley Books], John Wiley and Sons, 2012.

There are many commercial plasma torches available. Some examples are as follows: (i) low-power one-cathode torches, such SG100 (Praxair, Indianapolis, IN, USA) or F4 (Oerlikon Metco, Pfäffikon, Switzerland), (ii) low-power three-cathodes, such TriplexPro-210 (Oerlikon Metco, Pfäffikon, Switzerland), (iii) high-power torches. The high-power torches include e.g., Plazjet (Praxair, Indianapolis, IN, USA), Axial-III (Northwest Mettech, Surrey, BC, Canada), WSP-500 (IPP-ASCR, Prague, Czech Republic), and Delta-Gun (GTV, Luckenbach, Germany). These torches operate with the electric power input up to 200 kW. The low-power torches operate with the power up to 80 kW. The powder feed-rate can reach in high-power torches 100 kg/h.

Generally, the powder is injected radially, with injection angle ranging from 75° to 120° with regard to the torch axis. Only the Axial-III torch has injection angle of 0° i.e., axial injection. The injectors are mainly outside the plasma torch. Some troches, as e.g., SG-100 have a possibility to inject inside the torch. The flow-rate of the plasma gases vary from 40 up (low-power torch) up to 450 slpm (high-power plasma torch) [1,10].

The powders sprayed by APS method are most frequently oxide ceramics, such as Al_2O_3, TiO_2, Cr_2O_3, ZrO_2, Y_2O_3 as well as their alloys and their mixtures [15–17]. On the other hand, some of non-oxides ceramics can also be sprayed by APS, namely carbides, nitrides, and borides [18,19]. Similarly, the cermet coatings can be APS deposited [20–22]. A typical image of the powder feedstock, as well as manufactured coatings by APS method is presented in Figure 3.

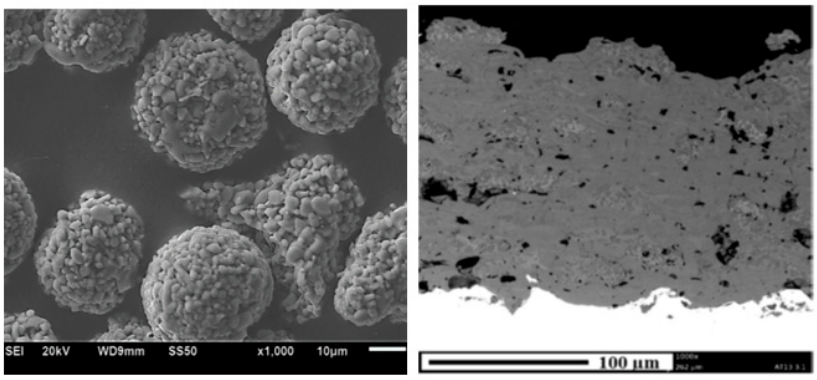

Figure 3. SEM image of Al_2O_3 + 13 wt.% TiO_2 powder (**left**) and APS coating sprayed therewith (**right**) [23].

The typical adhesion strength of air plasma-sprayed coatings is in the range from 15 up to 30 MPa. When, the bond coat is used (such as Ni-Al or Ni-Cr or Mo), the adhesion is higher and may reach 70 MPa. APS coatings may be of low (a few %) or high porosity (more than 20%), depending on the processing parameters. Typical coatings' thickness is a few hundreds of micrometers [1].

2.2. Suspension Plasma Spraying (SPS)

One of the serious limitations of conventional, powder-based, thermal spray technologies is the processing of fine powders. Small particles of low density materials are difficult to inject into high-energy jet or flame [24,25]. This means that obtaining submicro/nano-grained coatings is also limited. In order to overcome such problem, the innovative idea of using suspensions instead of dry powders, was patented by Gitzhofer et al. in Sherbrook University, Canada, in 1997 [26]. The patent describes that fine solids may be mixed with appropriate solvent (usually water or/and ethanol) and shows the chemical agents necessary to formulate a stable liquid feedstock.

The main advantages of the suspension plasma spraying (SPS) technique, shown in Figure 1, are as follows [8]:

- Feedstock transport from feeder to torch or gun is easy and may be realized under action of compressed gas pushing the liquid;
- Injection may be realized by atomized or continuous liquid stream (see Figure 4), creating the possibility to influence the coating's microstructure;

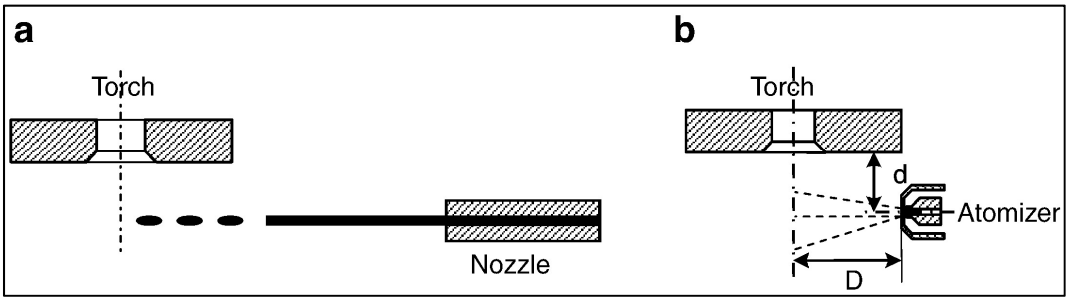

Figure 4. Injection of liquid using continuous stream, (**a**) and atomized stream, (**b**), after [8]. Reproduced with permission from [Surface and Coatings Technology], Elsevier, 2008.

- Fine powders may be more easily introduced to flame or jet in form of droplets;
- Solvent may provide some protection for fine particles against a direct contact with high temperature of flame or jet.

The use of SPS is advantageous for deposition of functionally graded coatings. The process offers the possibility to design the microstructure (see Figure 5) for example:

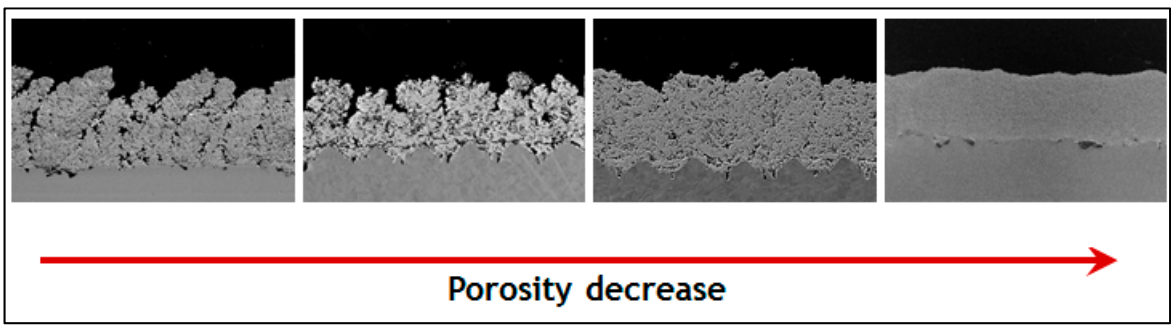

Figure 5. Various microstructures of YSZ coatings produced by SPS, after [27]. Reproduced with permission from [Advances in Materials Science Research], Nova, 2016.

- Coatings may be extremely porous (even more than 50 vol.%) or very dense (1–2 vol.%) [28–30], depending on the phenomena occurring in the plasma jet (see Figure 6);

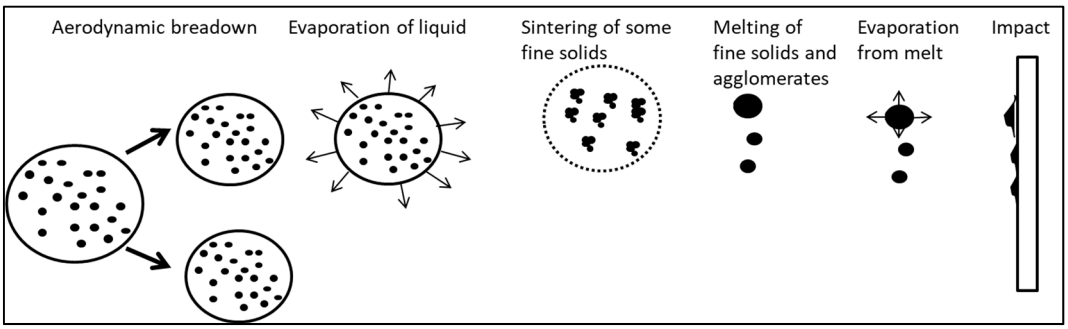

Figure 6. Phenomena occurring after injection of suspension droplet into plasma jet [14]. Reproduced with permission from [Wiley Books], John Wiley and Sons, 2012.

- Pores may be of nanometer, submicrometer, or even micrometer size, having various shapes and forms connected or non-connected networks [28–35];
- Morphology may vary from dense and homogeneous one, through vertically cracked up to fully columnar [28–30];
- Deposits may be formed by fully molten splats, sintered particles only, or by both as so-called *two-zones structures* [36,37];
- Roughness of coating's surface may vary in a very broad range (as reported in [35], R_a values may be between 1.6 and 14.1 μm);
- Thickness may be as low as a few micrometers and reach hundreds of micrometers [38,39].

Over the past years, many promising examples of using SPS technology in manufacturing functionally graded coatings were presented. One of the most studied topic in that field concerns bioactive coatings [40]. Cattini et al. studied in the Universities of Limoges and of Modena bioactive glass/hydroxyapatite (HA) functional coatings with various designs, namely: composite, duplex, and graded coatings [41,42]. Tomaszek et al. [43] studied SPS titania-hydroxyapatite functionally graded coatings. In this design, the TiO_2 layer was used as a bond one on Ti alloy substrate.

Thermal barrier coating (TBC) is another example of functionally graded coating system that can be sprayed by SPS. Björklund et al. [44] described the possibility of using hybrid plasma spraying concept to avoid sharp interface between oxidation/corrosion-resistant NiCoCrAlY bond coating and thermally insulating 8YSZ top coating. The hybrid spraying consisted of the manufacturing of bond coating by APS and the top one by SPS. Wang et al. [45] proposed the concept of graded double ceramic insulation layer in which 8YSZ and $La_2Zr_2O_7$ coatings were deposited by SPS.

2.3. Solution Precursor Plasma Spraying

The solution precursor plasma spraying (SPPS) allows manufacturing coatings with submicrometer and nanometer structures. The first research groups that used solutions for thermal spraying were from Stony Brook University, USA and Tampere University in Finland [46–50]. The evolution of SPPS method, starting from spray pyrolysis is described in [51]. The initial studies showing good quality SPPS coatings were reported in [52,53]. Subsequently, many coatings for different applications were sprayed by SPPS. The examples are: thermal barrier coatings (TBC) [54,55], coatings solid oxy-fuel cells [56,57], biomaterial coatings [58,59], photocatalytic coatings [60,61], coatings for gas sensors [62,63], environmental barrier coatings [64], and many others.

Both techniques, SPS and SPPS use liquid feedstock. Nevertheless, in SPS method, there are some solid particles suspended in liquid solvent. As the solids have small dimensions, the probability of their agglomeration at spraying is very high (see Figure 6). Also, the sedimentation of feedstock during

storage can be a serious problem. These problems are negligible for SPPS method, which uses purely liquid feedstock. Such feedstock is suitable to obtain coatings with very fine microstructure [65,66]. The solution precursors are easier to obtain with high purity, without contamination occurring frequently at suspension preparation [67].

The composition of deposited coatings changes the initial feedstock [68]. This change is easy to carry out in SPPS technology. Consequently, it is possible to enlarge the area of thermal spray applications [69]. Another important technological advantage is the possibility of using conventional plasma spray equipment. Also, the solution feeder in SPPS can be the same as suspension feeder in SPS technique [70].

The precursors used to spray are generally the mixtures of compounds, such as salts, acetates, or nitrates. The mixtures are dissolved in a solvent to form final solution. The solvent is frequently an organic liquid or/and water. It should be stressed up, that the mixing of the precursors occurs on the molecular level [71,72]. More details about solution precursor preparation are described in next chapter.

The schematic presentation of SPPS set-up is shown in Figure 1. There are many process parameters that influence the coatings microstructure and properties [73,74].

The phenomena occurring at SPPS process are shown in Figure 7. More details about these phenomena as well as interactions between droplets and plasma jet can be found in [51,68,75–80].

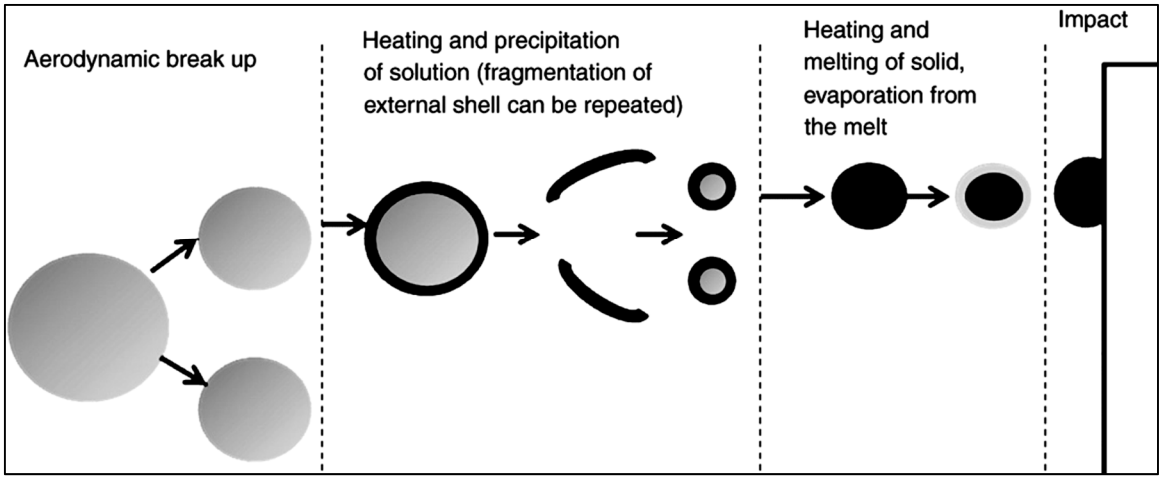

Figure 7. Phenomena occurring in plasma jet during SPPS process [75]. Reproduced with permission from [Surface and Coatings Technology], Elsevier, 2009.

Recently, the hybrid processes of thermal spraying were studied. There are two possible hybrid processes which include solution precursor plasma spraying, namely: (i) APS and SPPS shown by [81]; and, (ii) SPS and SPPS [82]. These processes take a profit from the advantages of both methods for new applications.

The SPPS method is a novel process that allows manufacturing a nanometer-scale coating, which results in many interesting functional properties impossible to reach in APS-deposited coatings. The advantages of this method are: pure feedstock with controlled chemical composition and different coating's microstructure adapted to application. The main drawback is the process complexity being more difficult to optimize than the conventional APS. The numerical studies may help in better understanding the phenomena occurring at SPPS method [77,83,84]. More details about the methods can be found in [51,70,84–87].

2.4. High Velocity Oxy-Fuel and High Velocity Air-Fuel Spraying

HVOF (high velocity oxy-fuel) and similar processes such as HVAF (high velocity air fuel) (see Figure 8) or HVSFS (high velocity suspension flame spraying) use gas combustion as energy

sources for melting and accelerating powder particles. The HVOF process enables reaching higher particles velocity and lower particle temperature than APS. Consequently, the process is characterized by high deposition efficiency, good adhesion of coatings, which have low content of oxides and low porosity [88]. In spite of relatively low deposition temperature, the thermal stresses are still present in the deposited coatings. This is the main reason for applying functionally graded coatings, FGC [89]. The FGC enables gradual change in coefficient of thermal expansion (CTE) and in Young's modulus which decreases stress level and increases bond strength. The FGC are particularly useful in reducing thermal stresses in thick deposits [89]. Hardness and ductility are the HVOF coatings properties which are often tailored to avoid the brittle breakup of coating's spallation [90]. The FGC may be obtained by: (i) using premixed powders or (ii) co-injection of different powders [91,92].

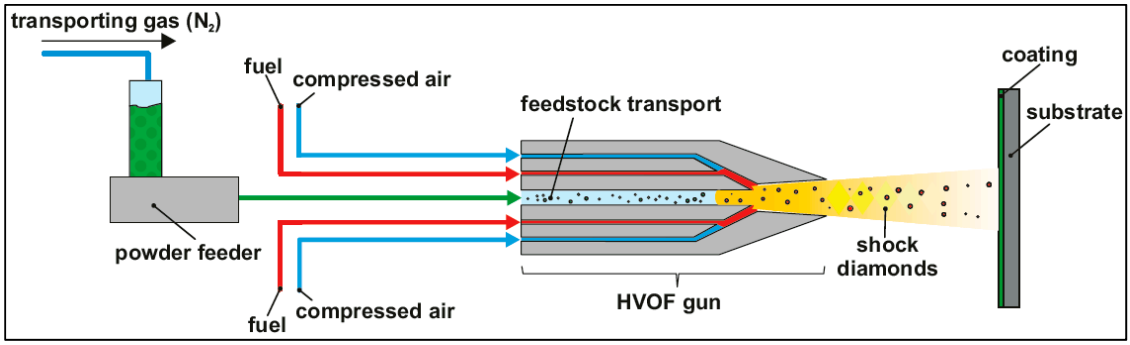

Figure 8. Scheme of high velocity oxy-fuel spraying, inspired by [1]. Reproduced with permission from [Wiley Books], John Wiley and Sons, 2008.

To show an example, Bolelli et al. [93] used the blends of powder with different compositions to deposit three graded coatings including WC–Co/NiAl. However, the co-injection of different powders seems to be more beneficial because the spraying process is continuous and the effort of powder preparations is reduced. Different ways of simultaneous powder co-injection are feasible such as e.g., the use of: (i) commercial twin powder feeder; (ii) two separate commercial feeders; and, (iii) modification of commercial feeders by the users. For example, Hasan et al. [94] designed and manufactured gravimetric powder feeder based on two separate powder chambers and control valves. The authors used it to spray the mixture of steel with aluminum. Zimmermann et al. [95] used separate powder feeders having modified injecting system. The injectors were evenly spaced in the feeder and the powder was injected radially.

In case of significant differences between the injected powders, it is possible to vary the location of powder injector with regard to the torch. For example, Ivosevic et al. [96] used two separate powder feeders with internal and external injection in order to adapt the spray process for the polymer and cermet powders having very different properties.

Among the parameters influencing the deposition of FG, the most important are spray distance and working gases (fuel and oxygen) flow-rate [97]. The coatings quality can be controlled by the control of the particles in-flight temperature [98]. Moreover, in case of FGC it is suggested to control the powder with the lowest melting point in order to avoid excessive evaporation [99].

Prchlik et al. [91] compared behavior of atmospheric plasma-sprayed Mo-Mo_2C/stainless steel and HVOF-sprayed WC-Co/stainless steel functionally graded coatings. An improvement of wear resistance was observed for plasma sprayed coatings. This parameter was not improved for HVOF sprayed coating. However, these coating had better resistance against crack propagation.

Schulz et al. [100] used HVOF to deposit the FGC of aluminum/tool-steel. The authors found the optimal number of layers to reach desired hardness and residual stresses level. Bolelli et al. [93] provided a comprehensive study about Ni-5 wt.% Al/WC-12 wt.% Co functionally graded coating. The authors observed an increase in crack resistance in FGC in comparison to the standard coatings.

Zimmermann et al. [95] showed that gradual coatings design brings advantages also for bond coats. The authors added the second powder to increase the ductility of MCrAlY at the temperature of 600 °C.

Hydroxyapatite coatings are usually deposited using APS. However, HA decomposes at high temperature deteriorating the coatings properties. As the temperature of the HVOF flame is lower than that of plasma jet, it may be considered as a promising alternative for APS. The technical solution would be an application of FGC to avoid stresses and the failures at the interface HA coating – Ti substrate. The HA/TiO_2 graded coatings on Ti implants seem to be a possible system to reduce the: (i) Mismatch of CTE values and resulting thereof temperature gradients between the HA coating and Ti substrate; and, (ii) risk of ions diffusion from the substrate to humane body [101].

The study of Yao et al. [102] showed the application of high velocity suspension flame spraying (HVSFS) for the deposition of multi-layered HA/TiO_2 coatings. The authors found out that the use of HA/TiO_2 improved adhesion of the coatings to the substrate.

2.5. Low Pressure Cold Spraying and High Pressure Cold Spraying

A main advantage of cold spraying is the low processing temperature compared to other thermal spray processes [103,104]. Instead of high thermal energy, the kinetic energy of gas is used to deposit powder particles, which deform the substrate [105,106]. The low gas temperature in cold spraying has some advantages, such as reduction of oxidation at spraying [107,108], avoiding of phases transformations, and reducing coating porosity [109,110]. The compressive stresses resulting from peening effect at impinging of solid particles enable deposition of many different metals and alloys [111].

The high kinetic energy at impact with substrate results from very high particles velocity. The particles are accelerated by working gas, as nitrogen, helium, or air, to reach the supersonic velocities. The working gases are pushed through de Laval type nozzle of the gun. The initial pressure of working gas enables categorization of cold spraying method as: (i) high pressure cold spraying, HPCS (gas pressure > 1 MPa); and, (ii) low pressure cold spraying, LPCS (gas pressure < 1 MPa). HPCS (see Figure 9) uses usually nitrogen or helium as the working gas. A stream of carrier gas passes through a powder feeder and transports powder to the gun. The powder is injected axially into the gun's nozzle. The working gas is heated before reaching the nozzle. The heating leads to an increase of the powder particles temperature which favors plastic deformation of particles upon impact. LPCS (Figure 9) operates with nitrogen or air supplied by a compressor. The gas is also heated prior to arriving to the gun. The powder is injected radially to the gun's nozzle. The LPCS installation is much cheaper in equipment price and processing costs than the HPCS one [112]. On the other hand the sprayed particle reaches much lower velocity than that in HPCS installation. Therefore, the application of LPCS is significantly limited to deposit the easy-plastic-deformable materials such as tin, zinc, copper, aluminum, and nickel. The deposition of composites as the cermets is also possible and becomes increasingly frequent [113].

One of the current trends in cold spraying is the manufacturing of multi-coatings as FGCs in additive manufacturing [114]. The FGC obtained by cold spraying use a mixture of: (i) different metal powders; or, (ii) metal with ceramic powders. The mixtures can be prepared by (see also Figure 10): (i) mixing of powders, (ii) mechanical milling followed by agglomeration and by sintering; and, (iii) powders cladding.

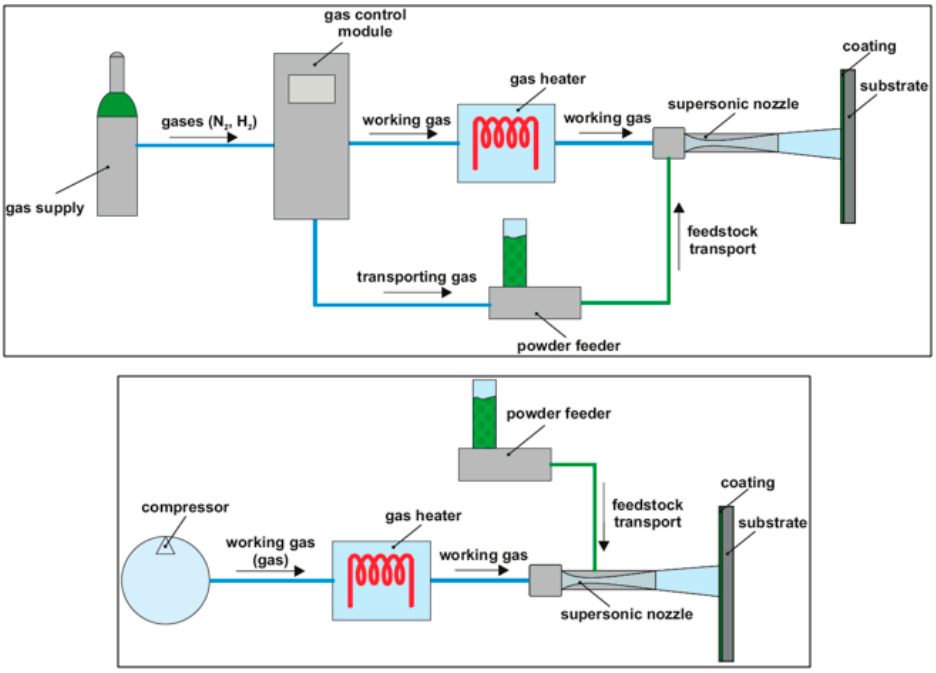

Figure 9. The scheme and principle of high- (**up**) and low-pressure (**down**) cold spray systems.

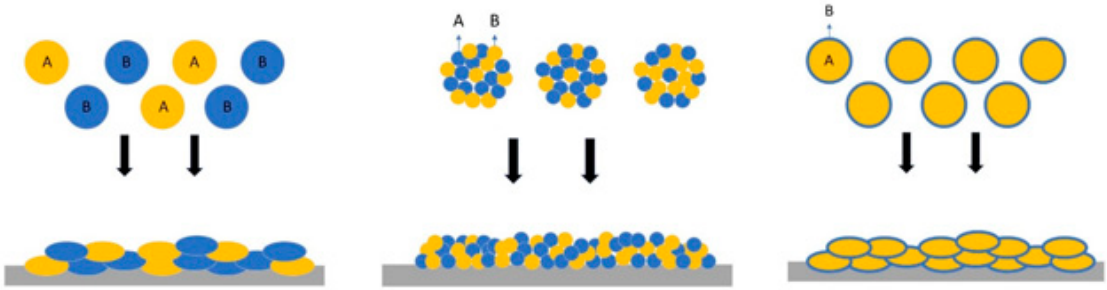

Figure 10. Methods of powders preparation in composite coatings deposition: mixture of powders (**left**), mechanically blended powders (**middle**), and cladded powders (**right**).

The mixing of powders having particle size of −50 + 5 µm is the most popular feedstock preparation method in cold spraying [115,116]. The HPCS enables better coatings properties to be achieved. On the other hand, the LPCS is the cheapest method enabling cermet coatings to be obtained. Therefore, a lot of recent studies deal with deposition of metal matrix composites (MMC). The papers describe the characterization of Al_2O_3 cermets with metals as Al, Cu, Zn, Sn, and Ni [117–120]. The MMCs coatings can have various applications. Their frequent function is regeneration of surfaces [121], electrical conductivity [122], corrosion resistance [123], wear resistance [124], biomedical [125], etc. These coatings combine elevated wear-resistance, machinability, and reasonable thermal conductivity. A low cost of technology makes it an attractive alternative to deposition of the complex and expensive alloys. The composite powder mixtures can be used in both HPCS and LPCS. The cold sprayed coatings have useful properties. To give an example, Winnicki et al. [126] deposited 3 mm thick Al + Al_2O_3 coating onto steel and measured the microhardness varying from 84 HV0.3 at the interface with substrate up to 130 HV0.3 on the top of the coating (see Figure 11). Consequently, the coating is hard on its surface being ductile at its interface.

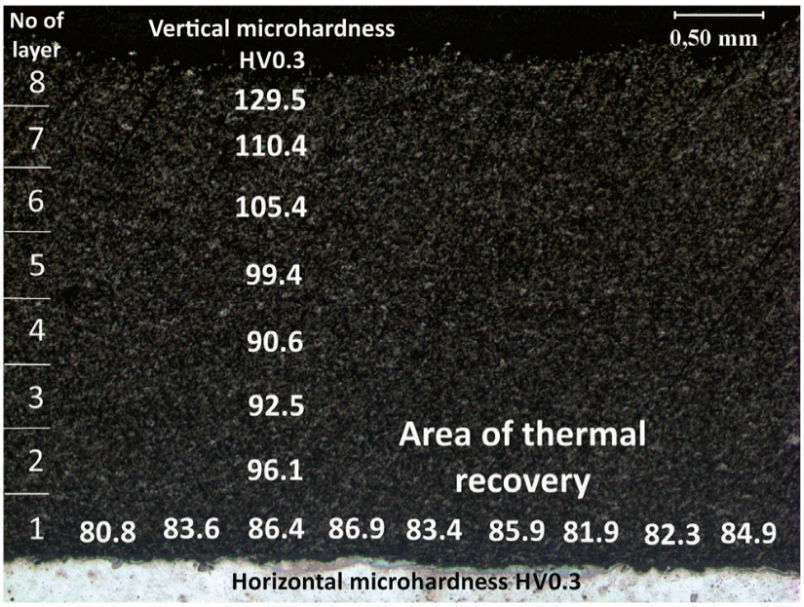

Figure 11. Microhardness distribution in the Al + Al_2O_3 composite coating obtained by LPCS [126]. Reproduced with permission from [Archives of Civil and Mechanical Engineering], Elsevier, 2016.

Many reports show advanced technology of functionalization of the coatings sprayed using mechanically alloyed powders. This powder production technology enables introducing the crystal refinement strengthening effects in the composite powders. Luo et al. [127] found that the grain size of the NiCrAl matrix in the c-BN–NiCrAl composite powder prepared by mechanical alloying had a size of a few tens of nanometers. Cold spraying enables preserving these small crystal sizes in coatings. The contributions of the strengthening mechanisms including work hardening, dispersion strengthening, and crystal refinement enabled reaching the hardness of cold-sprayed coatings of 40 vol.% c-BN + NiCrAl as high as 1175 HV [128]. Finally, hardness and many other properties can be increased by using nanostructured coatings obtained from nano-structured powders.

The mechanical alloying method of powder production renders more uniform distribution of ceramics in composite coatings. However, the spray process modifies the strength of the metal particles and its morphology which becomes more irregular and lowers the deposition efficiency. To resolve this problem an innovative process was developed. The process deals with the core-shell powders morphology. The core includes a reinforcing ceramic phase and shell is a ductile metal or alloy [129,130]. Feng et al. [130] compared a coatings properties obtained by spraying of powders obtained by mixing of ceramics and metallic powders with those obtained with powders having particles coated with CVD. The authors used Ni-coated B_4C composite to deposit composite coatings. They found that coatings obtained by mixing the initial powders results in coatings having B_4C content always smaller than 20 vol.%. Many B_4C particles were fractured. The coatings sprayed with CVD-coated powders particles had higher content of entire B_4C particles. Similarly, Yin et al. [131] compared the coatings cold sprayed using powder with particles of diamond coated with Cu-Ni with the deposits obtained using diamond particles mixed with the Al ones. The authors found, that the core-shelled diamond particles were easier to spray than that of powders mixture.

2.6. Post Spray Treatment

The as-sprayed coatings need frequently a treatment after deposition to meet the specifications. The treatment can be useful in: (i) obtaining the final dimension; (ii) improving the properties (especially wear-, corrosion resistance, and adhesion strength); (iii) modifying coatings' microstructure (decrease porosity level and increase homogeneity); (iv) reducing the residual stresses or oxide content;

and, (v) polishing the coatings' surface. Generally, post-spray treatment can be mechanical, physical (including heat treatment), and chemical. There are also combined processes [1,132].

2.6.1. Mechanical Treatment

The mechanical post-spray treatment is applied in order to obtain specified coatings thickness and to reduce the surface roughness. The processes, which can be applied, are turning, grinding, polishing, and lapping. The choice of treatment's technique depends mostly on coating material. The mentioned mechanical post-spray treatments are most frequently used to reduce the roughness of as-sprayed deposits which improves also their tribological properties [133].

Another important method is shot peening. This treatment is used in order to improve the fatigue resistance of coatings. It generates compressive stresses at their surfaces. Also, it allows closing the open porosity and flatten coating's surface. Similar treatment is rolling [134]. The examples of the shot peening application are described by [135,136].

Recently, the modeling of the mechanical post-spray treatment was developed to predict roughness and surface properties [137,138]. Finally, there are many, less frequently used methods of mechanical post-spray treatment such as buffing, hand stoning, tumbling, and burnishing [132,139].

2.6.2. Heat Treatment

The post-spray heat treatment is carried out mainly in furnaces under the operating temperature lower than the melting point of the coating material. During such type of treatment, diffusion and stresses relaxation take place. The first one may result in the improvement of the bond strength and in enhancing the inter-particle cohesion in coatings. The latter improves their wear and corrosion resistance. Moreover, the heat-treated coatings may become more ductile and may have greater fracture toughness and elastic modulus. On the other hand, the hardness of heat-treated coatings decreases and crystal grains grow-up. It is possible to carry out the heat treatment under controlled atmosphere or in vacuum. Other type of the heat treatment is remelting the sprayed coating. The details of such processes could be found in [1,132].

The remelting of coatings can be carried out using: laser beam [140,141], electron beam [142,143], and, electric arc [144,145]. The laser treatment that is most frequently used is described in detail in [146].

2.6.3. Chemical Treatment

The most frequent goal of chemical treatment is to close open porosity in as-sprayed coatings. The impregnation is a useful method. The impregnation consists of application of liquid sealants, which penetrate inside the coating by capillary actions, fulfilling the pores and solidifying thereafter. The sealing protects coatings and substrates against actions of corrosive media. There are three methods of impregnation, depending on the applied sealant pressure: low-pressure, atmospheric, and high-pressure. It is also possible to combine these methods [1,10,132]. The details of sealing methods and the parameters are described in [147]. The sealants may be organic [148,149] or inorganic [150,151].

2.6.4. Physical Treatment

There are two methods belonging to physical treatment: physical vapor deposition (PVD) and ion implantation [152,153]. The improvement of the coating's properties was slightly greater at ion implantation. However, this treatment is more expensive than the PVD one.

2.6.5. Combined Treatment

Hot isostatic pressing (HIP) combines two treatments by using simultaneously high temperature and high pressure (up to 300 MPa). The temperature of treatment depends on material type being in the range of 0.7 to 0.8 $\times$ T_m. This treatment is carried out in vessels under the inert atmosphere, mostly in argon [1,10]. The HIP allows improving adhesion strength as well as corrosion resistance

of the coatings. Moreover, it may enhance fracture toughness and reduce the residual stresses. Nevertheless, this treatment is limited in application to rather small sized pieces and is relatively expensive [154]. The HIP treatment is used mainly for ceramic and cermet coatings [155,156] and less for alloy ones [157–159].

Another combined process, in which temperature and pressure act simultaneously, is spark plasma sintering. The temperature is up to 1800 K and pressure up to 50 MPa, being lower than in HIP process. The principle of spark plasma sintering bases on the Joule effect caused by electronic and ionic conduction. The main advantage of such sintering is short treatment time, being shorter than that of HIP. The size of the treated piece is limited [1,154]. The spark plasma sintering treatment is used for ceramic, cermet, and composite coatings [160–162].

2.7. Feedstock Used in Thermal Spray Processes

The progress in TS technology and the establishment of new deposition methods resulted in an intensive development in feedstock used to spray.

The micrometric powders are frequently used in thermal spraying. The powders have chemistry, morphology, and size distribution tailored to spray method and to the application of coating [132,163]. Currently, the powders are made of different materials such as metals and alloys including intermetallic alloys, ceramics, polymers, and their composites. The market of powders is open and there are companies or R&D centers, where the desired powders may be produced on demand.

The physico-chemical properties of powders, including e.g., melting point, crystallinity, heat conductivity, coefficient of thermal expansion or specific result from their chemical composition. However, the production route significantly influences the powder characteristic such as particle morphology, size distribution, and apparent density [164]. The most important powder manufacturing processes are [1,165]: (i) atomization (gas or water); (ii) fusion or sintering followed by crushing; (iii) agglomeration by spray-drying; (iv) cladding; and (v) mechanical alloying. The selection of powder material suitable for a specific coating requires understanding of the application, customer requirements, and environment at coating's service. Furthermore, the feedstock should be appropriate for the specific thermal spray technology. The smallest size of powder particle sizes is generally and for all spray techniques about 10 to 15 µm [164]. The greatest size depends a lot on the coating application. The value of 90 µm is a typical one used for APS and the value of 30 µm—for LPCS. The powders used in other spray techniques have the greatest sizes between these two values [164].

Generally, it can be assumed that spherical, free of internal porosity, chemically homogeneous, and having narrow powder particle distribution are the preferred ones for all TS technologies [165].

The latest developments in micrometric powders for thermal spray technology concern:

- New production methods, like small and flexible atomization plants where low amounts of completely new, often expensive, and high-quality powders may be produced [165–167];
- Powders with complex chemistry and controlled phase composition or even crystallinity, like amorphous metallic glasses [168–170], spinel powders [171], etc.

The introduction of nanotechnologies, observed starting from late 1990s resulted in the interest in the deposition of finely grained coatings [8,27]. The powders enabling deposition of such coatings can be prepared by [27,48,172]:

- Pre-agglomeration of very fine particles (see Figure 12) into micrometric powders and then careful control of spray parameters in order to melt the powder outer surface only to preserve fine-grained structure of the particles core;
- The use of a new class of liquid feedstocks, namely suspensions and solution, to change the interaction between the hot gases and feedstock in the way to enable obtaining finely grained coatings.

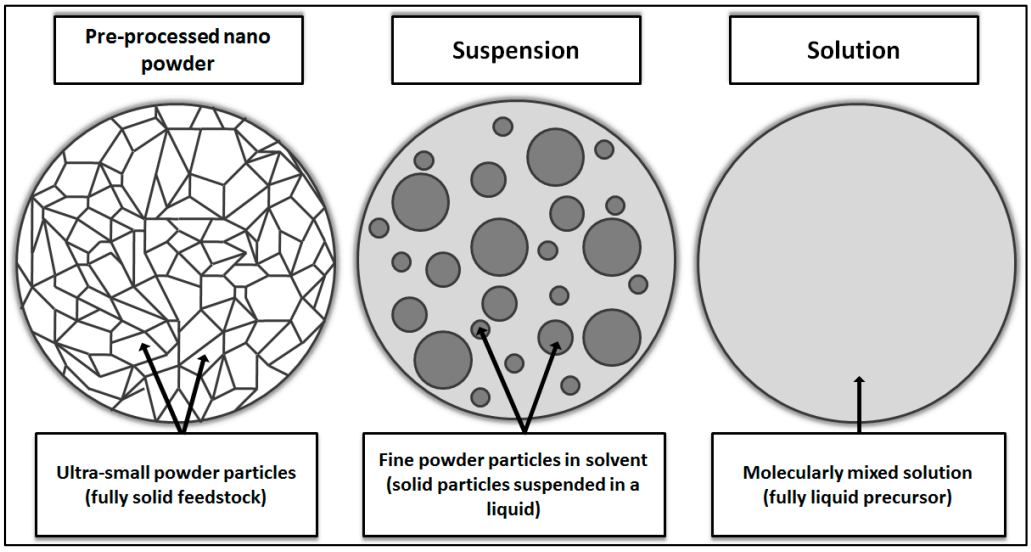

Figure 12. The feedstock used for deposition of finely-grained coatings by thermal spraying [27]. Reproduced with permission from [Advances in Materials Science Research], Nova, 2016.

A suspension is a homogeneous mixture of fine solid particles, solvent, and some chemical agents [27,75,173]. The powders are usually sub-micrometric or nano-metric in size. They may be prepared by a *top-down* approach such as mechanical milling of micrometric powders. Another possibility is the *bottom-up* way consisting in a synthesis from precursors having desired chemical composition. The content of solid in suspension used starts with a few wt.% but, for industrial applications the used concentration reaches 50–70 wt.%. The solvent plays a similar role as a carrier gas in conventional TS but may also prevent powder particles against high temperature. Water, alcohol, and their mixtures are mainly used. Finally, some chemical agents are added in order to formulate a stable suspension of relatively lower viscosity. The various flocculating agents are used for this purpose.

The suspension spraying is in its development stage and further innovation is required. Sokołowski et al. [174] suggested a way to develop suspension plasma-sprayed zirconia with columnar microstructure. Berger, Toma, and their group from Fraunhofer Institute in Dresden (Germany) suggested adapting the suspension properties to the final application of coating. Consequently, they proposed the multi-material suspensions [175–178]. Molina et al. [179] proposed the formulation of stable, highly concentrated, and low viscosity liquid feedstock with the use of bimodal or multimodal solid size distribution.

The solutions are another liquid feedstock. Their formulation starts with the solutes of salts, nitrates, or acetates being dissolved in aqueous or organic solvent. The solutions are mixed on a molecular-level and the desired stoichiometry of coating is reached at spraying. The high molarity of used precursors is preferable to increase deposition rate [75,174,180].

The solution precursor spraying is intensively developed and the recent study shows e.g., the compositionally graded and porosity graded coatings [181], doping of solution precursors by rare-earth elements [182] and by metal ions [183,184].

There is a possibility of spraying different feedstocks simultaneously, which is called hybrid spraying. The combinations of powder with suspension, powder with solution, and suspension with solution were tested [82,185].

3. Principal Properties of Thermal Spray Coatings and Methods of Their Characterizations

The TS coatings are frequently used in different branches of the industry. The industrial applications require specified properties, such as e.g., wear resistance, corrosion resistance, thermal shock resistance, biocompatibility etc. These properties help in qualifying the deposits for the applications [1,7,186].

This section describes briefly the mechanical, physical, and biological properties and their methods of characterization.

3.1. Mechanical Properties

The mechanical properties include mainly the bond strength, microhardness, elastic modulus, fracture toughness, shear modulus. Moreover, there are tribological properties such as e.g., wear resistance which are important, in many applications [1,10].

The properties result from [186]: (i) method of coatings manufacturing and the used parameters, (ii) material composition; and (iii) feedstock characteristics.

3.1.1. Adhesion (Bond Strength of Sprayed Coatings)

The state-of-the-art of coatings adhesion evaluation methods are shown by [186,187]. The most common method is tensile adhesion test (TAT), which is specified in the ASTM C633 (https://www.astm.org/Standards/A633.htm checked on 10 July 2020) or ISO 14916:2017 (https://www.iso.org/standard/60995.html checked on 10 July 2020) standards. The tests are used in research and in industry [1,7,10]. An example of application of TAT method could be found in [188]. The modification of conventional TAT test were proposed for flat and wide substrates. For example, Leigh and Berndt [189] developed single bar and double bar methods. There also are many shear tests useful in determining the adhesion strength [190–194]. Many tests of adhesion were developed basing on fracture mechanics [195]. Other methods of adhesion characterization in macroscopic and microscopic scale include the tests such as: tubular coating tensile, peel adhesion, pin, laser-shock, interfacial indentation, and scratch one [196–205]. The cohesive strength of a coating can be determined by tests of tensile adhesion, pin, shear load, and scratch one [206].

3.1.2. Hardness Measurements

Hardness is easy to measure and is very frequently tested. The hardness is material resistance to deform under load in the perpendicular direction to the investigated surface. The test is usually made by indentation technique as in the study [206]. Hardness correlates well with abrasive and wear resistance [207,208]. An indenter identifies the methods of measurements. The best known indenters are of Vickers and Knoop. Other indenter are: spherical, conical (Rockwell test), and triangular (Berkovich test) [208–213].

Another method for micro- and nano-hardness determination is an indentation test (IIT). This technique proposed by Oliver and Pharr [10,214] also gives information about such material properties as elastic modulus, elastic, and plastic work of indentation or even creep. IIT method enables taking into account the influence of pores and cracks on hardness and elastic modulus of coatings [215].

3.1.3. Elastic Properties

The elastic properties of thermal sprayed coatings are strongly dependent on porosity and inter-lamellar contacts [216]. This property helps in appreciation of coatings quality. The methods of elastic modulus testing can be divided based on destructive and non-destructive testing [1,209,214]. The destructive methods include indentation technique, which uses the cross section of samples. This method was developed by Marshal et al. [217]. The method useful for free-standing coatings is tensile or compression test developed for bulk materials. Finally, a destructive method is cantilever beam test, which can be made during and after coating's spraying [218–222].

The non-destructive methods include [1,223–225] laser acoustic test and ultrasonic spectroscopy one. These methods are very sensitive on defects in the coatings.

3.1.4. Fracture Toughness

The fracture toughness for thermal spray coatings can be characterized by strain energy release rate (GI_c) or fracture toughness (KI_c). The following methods are mainly used for the coatings [1,204,226–228]: (i) double-cantilever beam; (ii) double torsion; (iii) indentation test; (iv) bending test; (v) scratch test; and (vi) tensile test.

3.1.5. Tribological Properties

The most frequent wear is adhesive, abrasive, and erosive. The other types include: fatigue, fretting, oxidation, cavitation erosion, corrosive, and impact wear. Consequently, there are many tests methods enabling wear estimation described by [229–232].

The most frequently used tests estimate the adhesive wear. The tests are carried out with a tribometer, which may have following configurations: pin (or ball) on disc, pin on plate, block on ring. The abrasive wear can be characterized as two-body abrasion and three-body one. The latter is used more frequently [232–234]. The erosion wear describes surface damage by a fluid which includes solid abrasive particles [235–237]. Thermally spray coatings were investigated with the tests, which allowed determining fatigue, fretting behavior, corrosion and cavitation erosion resistance, and many other [238–242].

3.2. Physical Properties

The basic properties of coating are thickness and porosity. In general, TS technology may provide coatings having thickness of a few micrometers up to a few millimeters. Each spray pass introduces some thermal energy to the coatings structure, this results in correlations between thickness, residual stresses, and bond strength [243].

The design of FGCs may include gradients of porosity, density, and of pores size. Such gradients are useful especially in bio-coatings manufacturing, for bone implants. The dense structure near to the interface between coating and implant assures high adherence. The porous structure in the outer part of FGC promoted the in-growth of bone [244,245].

The physical properties, which are important for FGC include thermal transport properties and coefficient of thermal expansion (CTE) among many others [246]. These properties are important for thermal barrier coatings (TBC). Thermal transport properties include thermal diffusivity and thermal conductivity. The TBC includes, generally, two layers with metallic bond coat (BC) and ceramic top coat (TC). The layers have different thermal transport properties (low conductivity of the top coat) and different thermal expansion (high CTE of bond coat) [247,248]. The literature concerning TBCs is very rich and shows many data related to these two parameters [249–251].

The electrical properties of FGC include electron field emission. This emission of electrons from coating's surface occurs under action of strong electric field. The important parameter characterizing the field emitters is the electric field enhancement factor. The TiO_2 emitters were sprayed using the SPS method [252]. The sprayed emitters had similar parameters to nano-diamond and diamond-like films described in [253]. The electron emission of TiO_2, TiO_2/Al_2O_3 coatings depends on their temperature [254–256].

The dielectric properties of thermally sprayed ceramic coatings have been frequently tested. The electrical breakdown strength and dielectric constant of APS, SPS, and HVOF sprayed alumina were determined to be in the range 9–40 kV/mm and 5.3–8.3 respectively [257–261]. The breakdown strength of alumina was the highest for HVOF sprayed alumina coatings.

Titanium dioxide is used for photocatalytic decomposition of impurities found in water. Various toxic and hardly degradable compounds are broken down owing to the hydroxyl radicals. The research on the field was done to optimize the catalyst and its deposition on supports. Consequently, TiO_2 coatings were deposited on different substrates. The stainless steel substrates coated using SPS were studied by [262–264]. The photocatalytic activity of sprayed coatings was determined by measuring

the degradation of an aqueous solution of dye methylene blue. The photon efficiency of titania deposits was the measure of the photocatalytic performance and varied from 0.022% up to 0.032%. Titania coatings were also sprayed using HVOF method. The coatings were used to degrade phenol in the solution by authors of [265]. Finally, HVOF and APS techniques were used to spray titania coatings tested by decomposition of acetaldehyde [266].

3.3. Bioactivity and Simulated Body Fluid Corrosion Resistance

The important category of FGC are related to the biomedical applications. The properties useful in this application are: (i) bioactivity determining interface bonding between implant and bone tissue; (ii) micro-porosity which allows the osseo-integration; (iii) mechanical properties especially compressive strength, high wear resistance, and cracking energy; and (iv) corrosion resistance against body fluid [267–271]. The biomaterials can be divided by taking into account the compatibility with human body, on the following groups: bio-incompatible, bioinert, bio-tolerant, and bioactive.

As the methods of mechanical and physical properties characterization were described in previous sections, the present one is focused on the bioactivity. It should be stressed that FGC is obtained by using bioactive hydroxyapatite (HA) doped by Ag, Zn, ZrO_2, TiO_2. Another group of graded coatings uses bioinert Ti alloy sprayed with Al, V, Nb, Zr and with bioactive bioglasses [272,273].

3.3.1. Corrosion Resulting from Immersion in Simulated Body Fluid

The coatings including HA are frequently tested by immersion in simulated body fluid (SBF) at a temperature equal to 37 °C, with the pH value of the fluid equal to 7.4 [274]. This method is not expensive, making it possible to use for samples of different geometries. The drawback of the method is that SBF simulates only inorganic part of human blood without taking into account the presence of proteins, vitamins, glucose etc., [275].

Kokubo et al. [276] proposed the chemical composition of SBF. Many modifications of SBF has been proposed [275]. Other corrosion tests can be made using accelerated calcification solution, supersaturated calcification solution, and phosphate buffered saline [277–279].

The immersion times vary from few hours up to two months [280]. The coatings arecharacterized after immersion by scanning electron microscope (SEM) and X-ray diffraction (XRD) to observe the morphology of their surfaces and the phase composition evolutions respectively [281–283].

3.3.2. Immersing in Cell culture Medium

Before introducing a new biomaterial for clinical use, the *Cell culture* tests are required [284]. The *Cell culture* test uses the humidified atmosphere including 5% CO_2. The conditions, being used in *Cell culturing* simulate better in vivo environment than SBF medium. Consequently, the test enable better estimation of coating's biocompatibility. The test enables finding the changes in free energy and the rate of precipitates nucleation as well as the cell cytotoxicity [285,286].

4. Major Applications of Functionally Graded Coatings

The FGC are used as thermal barrier, biomedical and photocatalytic coatings, and coatings in printing industry. These applications are described in the present section.

4.1. Thermal Barrier Coatings

TBCs are the coatings designed to protect the gas turbine parts against intensive heat flux and various eroding and corroding particles contained in air and fuel [287,288]. The frequent TBC's configuration includes ceramic top coat (TC) and metallic bond coat (BC). Each layer, shown in Figure 13, has different role to play in protecting the gas turbine components. Two goals to reach by TBC are: (i) extension of the turbine lifetime in service; and (ii) increasing the operating temperature and the thermodynamic efficiency.

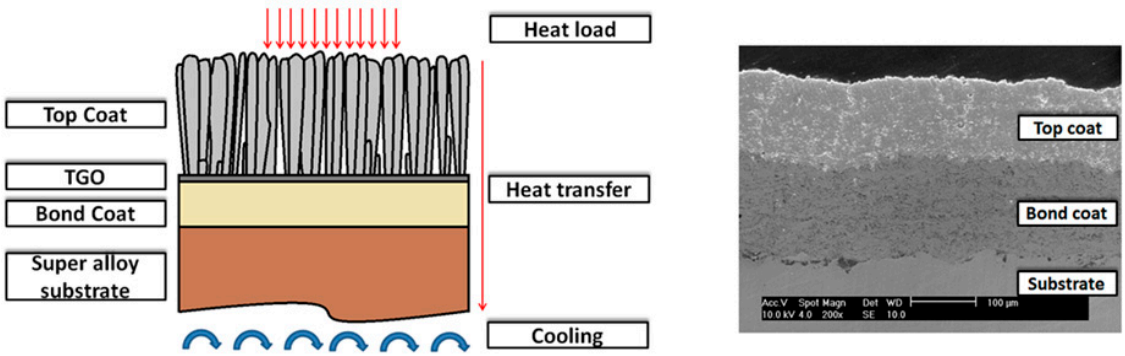

Figure 13. The schematic representation of TBC structure (**left**) and as-sprayed one (**right**) [27]. Reproduced with permission from [Advances in Materials Science Research], Nova, 2016.

The TC is exposed directly to the thermal, thermomechanical, mechanical, and chemical loads. This role of this coating is to protect the internal ones. The coating is of ceramics, being usually partly stabilized zirconia. The BC is composed mainly of MCrAlY alloy (M is metal as e.g., Ni, Co, Fe). Its role is the reduction of the CTE mismatch between TC and substrate. Another role is to protect the super alloy substrate against oxidation at high temperature. The BC contains aluminum, which diffuses forming a protective α-Al_2O_3 which is called thermally grown oxide layer (TGO). The TGO growth results in a generation of stresses at the BC/TC interface. These stresses reduce the time of TBC service [289,290].

TBC is a very well-known FGC system. The initial studies on the functionally graded thermally sprayed TBCs were performed more in the 1970s [291,292].

During the last years, because of the progress in spray technology and feedstock materials, two advanced functionally graded TBCs concepts were developed:

- ***First concept*** consists of gradual change from fracture-resistant BC layer to heat-resistant TC layer by initial mixing the feedstock powders or by injecting feedstock by different injectors. It resulted in a significant decrease of residual stresses and in improvement of adhesion between subsequent layers leading to the long-term performance of TBC [249]. The concept could be realized by mixing the zirconia and MCrAlY alloy powders and then spraying the mixtures [293,294]. The authors found out that some interlamellar discontinuities were formed in the final structure because of different properties of the mixed feedstock. Other authors used the mechanically pre-alloyed MCrAlY and 8YSZ powders with different ratios. The APS deposition of powders prepared in that way enabled high deposition rate, uniform coating density, and chemical homogeneity to be achieved [249,295]. The use of two injectors for 8YSZ and MCrAlY powders separately was another idea [296,297]. The coatings sprayed in this way were almost crack-free and their chemical composition changed gradually across the thickness without a distinct interface between layers. A new idea is the deposition of functionally graded TBCs using spraying of hybrid powder-suspension feedstock [44]. The authors report about gradual change of TBC microstructure from dense bond coat to columnar top coat. The TBC showed high resistance against oxidation at high-temperature test and high resistance against thermal shocks.
- ***Second concept*** consists of gradual change of chemical composition in TC. At least two different ceramics are used as layers. The outer one made of ceramics with high phase stability and low thermal conductivity, like e.g., alumina. The bottom ceramic layer should have high toughness, high fatigue performance, and low thermal conductivity. This specification corresponds to e.g., yttria stabilized zirconia such as 8YSZ [298,299].

There are several works focused on multi-ceramic TC in which YSZ is used as the bottom layer. The studies concerned:

- APS and SPS deposited 8YSZ/$La_2Zr_2O_7$ coatings [45,300];

- APS deposited 8YSZ/$Gd_2Zr_2O_7$ coatings [251];
- APS deposited $La_2Ce_2O_7$/8YSZ [301];
- APS deposited $LaMgAl_{11}O_{19}$/8YSZ bilayers [302].

The studies aimed at prolonged thermal cycling lifetime compared to the conventional two-layer TBC. The goal was reached owing to the increase of phase stability and of resistance against sintering.

A small modification was proposed by applying yttria- and ceria-stabilized zirconia (CYSZ) as bottom layer instead of yttria-stabilized zirconia (YSZ) [303,304]. The obtained FGC showed low thermal conductivity and satisfactory thermal shock resistance.

Finally, an interesting idea of depositing the YSZ layers having various microstructures was presented [305]. The bottom layer was dense to improve bonding and the external one was porous to decrease thermal conductivity.

4.2. Biomedical

Millions of different types of prostheses (of hip for example) are produced annually in the world; different biomaterials and various methods of manufacturing in production.

The major group of biomaterials include: (i) bioinert as titanium and its alloys; and (ii) bioactive as hydroxyapatite (HA) and bioglasses. The bioactive materials dissolve in human body, which accelerates the processes of prosthesis implantation in a bone [1,306]. The production of hip's and knee's prostheses, dental implants, and repairing of the bones are the major fields of activity [307].

Initial studies dedicated to application of FGC in biomedical applications were made by group of Khor [308–310]. The investigations aimed in obtaining well adhering and bioresorbable coatings. The use of TiO_2 as intermediate coating enabled to reach the tensile adhesion strength of the HA-TiO_2 system as high as 50 MPa [311]. Moreover, the use to titania bond coat increased the coating durability and improved fatigue resistance. Moreover, TiO_2 was a barrier for metallic ions migrating from metallic substrate to human body [312,313].

Another idea was APS deposition of titanium coatings with gradient of porosity [314]. The coating being in contact with substrate was dense; the middle one included micro- and macro-porosity and outer one was very porous to promote tissue growing. The authors [315] proposed the multi-coatings including HA-ZrO_2-Ti coatings by APS. The coatings with internal Ti coatings had reportedly satisfactory mechanical properties.

An important drawback of HA is its thermal decomposition at temperatures slightly below its melting point (depending of partial pressure of steam). This was the motivation to develop functionally graded structures, multi-coatings, hybrid organic-inorganic composites by using the oxides $CaO–P_2O_5–TiO_2–ZrO_2$ [316–318].

An important issue in FGC technology is optimizing the process parameters. The researchers often use the *response surface methodology*. This approach was proposed to design the graded HA coatings which should be [319]: (i) stable for long time; and (ii) bioactive. The intensive studies on FGC composed with HA, Ti, and TiO_2 used statistical methods to improve coating properties [320,321].

The frequently used thermal spray technique to manufacture biomedical coatings is APS. Other techniques were also tested. For example, Henao et al. [101] used HVOF to spray HA/TiO_2-graded coatings onto the Ti6Al4V substrate reaching satisfactory behavior at SBF testing. The use of FGC of HA and bioglasses was favorably compared with the conventional plasma-sprayed HA [322]. The improvement of mechanical properties of coatings was achieved by the use of the composites of HA or bioglasses by nano-diamond or reduced graphene oxide [323,324].

The SPS technology to spray FGC of HA and TiO_2 was used by the authors of studies [43,325]. They compared two configurations of coating: duplex and gradient one. These oxides were SPS deposited with the use of peristaltic pumps to inject the suspension (see Figure 1) resulting in relatively thin coatings [326].

The functionally graded coatings composed of bioglass and HA were produced by SPS [41,42]. The studies aimed at combining rapid osseointegration of bioglass with long term stability of HA.

The obtained coatings were immersed in SBF and exhibited strong reactivity with the medium. The authors produced all coatings by exclusively SPS technology or, by using APS technology to spray HA and SPS one to spray bioglass.

The suspension was also used as a feedstock in high velocity oxy-fuel spraying by Yao et al. [102]. The authors manufactured multilayer HA/TiO_2 coatings and improved the mechanical properties of deposits such as adhesion and wear resistance with regard to pure HA coating.

The high quality FGC biomedical coatings have an important potential in medical applications. The group of biomaterials for coatings, namely hydroxyapatite and bioglasses exhibit good in vitro as well as in vivo biocompatibility. The FGCs in biomedical applications allow improving osseointegration and reducing the shear stresses occurring at the bone–implant interface. The long-term stability of the FGCs and the stability of their biocompatibility still remain to be improved in future. The statistical methods may help to understand better the phenomena occurring in contact of coatings with the human body [321,326].

4.3. Photo-Catalysis

Photo-catalysis is an important issue in the chemical industry being related to degradation and destruction of organic pollutants. Fujishima and Honda [327] were the first to describe this phenomenon. More details are presented in the studies [328,329]. Thermal spraying technology works on three semiconducting oxides, namely TiO_2, ZnO, and SnO_2. TiO_2 seems to be most frequently tested [1]. An important point is the fact that at the photoreaction the surface of oxide remains unchanged [330]. The possible applications of the photocatalytic thermal spray coatings is the self-cleaning of surfaces (e.g., glass building). The photo-catalysis was also tested for water and air purification, for anti-fogging surfaces, for photo-catalytic lithography, and for many other applications [331,332].

An example of composite photo-catalytic coating used against air pollution is TiO_2 doped with Fe_3O_4 coating sprayed on mild steel substrates [333,334]. Because of the presence of intermediate phases, such as $FeTiO_3$, the band gap is narrower, than in pure TiO_2 which resulted in better photocatalytic activity with reported efficiency of more than 90%. Inversely, the nanostructured TiO_2/Fe_3O_4 plasma sprayed coatings did not exhibit satisfactory photocatalytic properties. Their best photocatalytic efficiency was as low as 23%. Chen et al. [335] sprayed the coatings of TiO_2 doped with ZnO or CeO_2 or SnO_2 on the foamed aluminum substrate and used them for benzene degradation. The coatings doped with CeO_2 and SnO_2 degraded better than that doped with ZnO. Nevertheless, their efficiency was greater than 90%. Ctibor et al. [336] sprayed titania doped with iron coatings. The coatings were used for butane decomposition under visible and UV radiation. The photocatalytic activity was also observed in plasma-sprayed TiO_2 + ZnO.Fe_2O_3 coatings [337]. The photocatalytic efficiency was promoted by $FeTiO_3$ phase being present in the coatings. On the other hand, the large amount of $ZnFe_3O_3$ phase was not favorable for the photoactivity. The innovative plasma-sprayed composite of TiO_2 with carbon nanotubes had photo-catalytic activity greater than pure TiO_2 deposits [338].

Robotti et al. [339] deposited TiO_2 with ECTFE polymer composite coating by LPCS method. The coating was used to degrade of NO and NO_2 pollutants. The photocatalytic activity of obtained coatings were much better than that of commercial paint.

The group of Hua Li from Ningbo, China [340,341], manufactured nanocomposite coatings of TiO_2/HA and TiO_2/HA/reduced graphene oxide obtained by flame spraying and tested for water disinfection and air purification.

4.4. Applications in Printing Industry (Corona and Anilox Rolls)

The APS method is widely used to spray coatings in the printing (*anilox rolls*) and packaging (*corona rolls*) industries.

Anilox rolls are used to transfer ink to paper at printing. The ceramic coatings sprayed with the APS method replaced galvanic layers used previously. The specifications of coatings in such rolls are hard to realize. Namely, the surfaces of coatings must be smooth, free from defects, resistant to abrasion and

corrosion, with high wettability [132,342]. The rolls are made of stainless steel. The metallic bond coat is sprayed on the substrate followed by a ceramic, mainly Cr_2O_3, top coat. The as-sprayed coatings are ground and polished. The laser engraving of small cells follows. The last stage is the final polishing. There is a tendency to increase the density of cells on the surface. The rolls with the surface texturing after spraying are also sometimes used [343]. The rolls are important and increasing part of thermal spray market [344]. It should be stressed up, that anilox rolls can be produced with other than Cr_2O_3 oxides such as e.g., Al_2O_3 + TiO_2 alloys [345]. On the other hand, the Cr_2O_3 coatings can be produced with use of HVOF spraying [346].

Corona rolls are used to increase the adhesive capacity of printing ink to the polyethylene surface by the use of plasma generated at corona discharge. The rolls used in the process were coated by Al_2O_3 sprayed using the APS method. The amount of metal (The inclusions of metals in sprayed coatings are mainly the droplets of W or Cu from the spray torch electrodes.) in sprayed alumina must be as small as possible. Therefore, it is very important to optimize parameters and to control the electrodes of the torch. The coatings must have good dielectric properties and being thick enough to have high breakdown voltage [347]. This requires spraying of thick alumina coating. The APS-sprayed alumina coating on corona rolls can be sealed after deposition [348]. The rolls are an important part of the plasma spray set-ups market [349].

4.5. Other Applications

A rapid development of industrial technologies in the industrial sectors of aerospace, automobile, shipbuilding, etc., resulted in many applications of non-ferrous metals. Consequently, the joining of such metals became an important issue. The conventional welding processes are not adapted for joining the non-ferrous metals. A possible solution is an application of an additional interlayer. The popular techniques of interlayers deposition are hot dipping and galvanizing [350–352]. An interesting alternative is cold spraying technique. Winnicki et al. [353] used LPGS to deposit composite coatings of Al + Al_2O_3, Al + Ni + Al_2O_3 and Ni + Al_2O_3. The authors found that the microstructure of Ni + Al_2O_3 interlayer after the resistance spot welding (RSW) remains unchanged (Figure 14) and that the shear strength of the joint was comparable to that of joint of Al + Al. Another opportunity to use the cold spray technology was a deposition of interlayers on non-metallic substrates made by Wojdat et al. [354]. The authors used metallic (Al and Cu) and MMC composite (Al + Al_2O_3 and Cu + Al_2O_3) interlayers in soldering and concluded that the interlayers deposited by LCPS effectively limited formation of the reaction zones at the interface of interlayer with the soldered joint. Consequently, the mechanical properties of such joint could were improved [354]. Li et al. [355] used cold spraying to obtain Sn-Cu coatings onto aluminum and on copper substrates. The results showed the improvement in soldering. The deposition of graphite-copper composite coatings onto aluminum alloy 6060 with the use of LPCS were analyzed in [356]. The authors added aluminum, aluminum with alumina and copper to exclude erosion of the graphite at cold spraying of composite coating.

MMC coatings are used frequently to improve resistance against erosion and wear. Most of thermal spraying processes are done at high temperature and, consequently, are associated with the phase transformation, oxidation and decarburization of ceramic reinforcement or soft metal matrix. Therefore, a low temperature process of cold spraying can be useful. The drawback of cold sprayed MMCs is low strength and ductility. The post-spray heat treatment process may help in eliminating these negative effects. Consequently, the post-spray friction stir processing (FSP) of MMC coatings deposited by cold spray was tested [357–362]. Such post-treatment resulted in reduction of interparticles distance and in refinement of the reinforcing particles. Peat et al. [361] showed that FSP post-spray treated cold sprayed Al + Al_2O_3 composite coating had satisfactory erosion resistance.

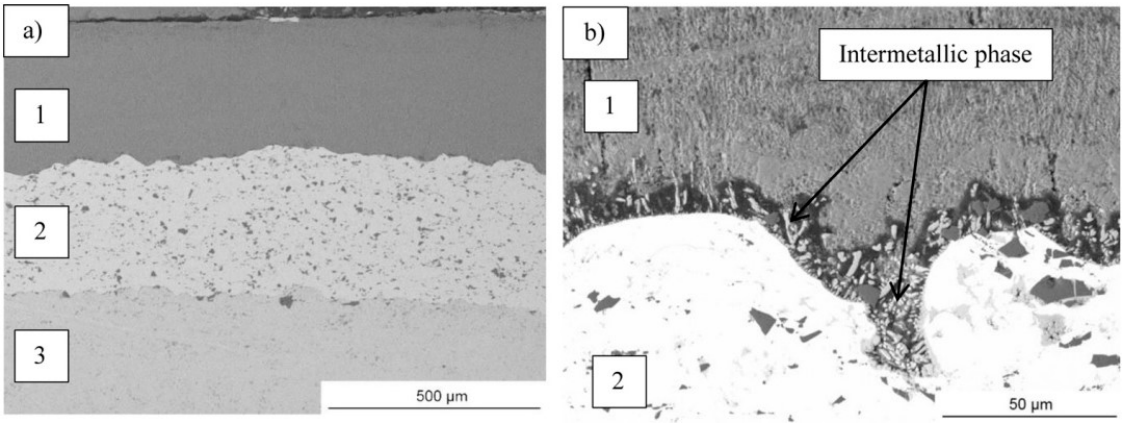

Figure 14. SEM-BSE micrographs of RSW aluminum—steel joint with Ni + Al_2O_3 interlayer (**a**,**b**). 1—aluminum alloy, 2—Ni + Al_2O_3 interlayer, 3—steel substrate [353].

5. Perspectives of Development of Functionally Graded Coatings

5.1. Polymers as Substrates

Polymer are attractive in many applications because of their small density and small CTE [363]. However, the exposure to harsh environment such as ultraviolet (UV) radiation, moisture, or high temperature deteriorates their properties. Consequently, some coatings protecting their surface were useful [364]. Thermoplastic polymers are easier to be coated than thermosetting polymers because of their thermal softening [365–367]. However, particularly interesting for industrial applications are polymer matrix composite (PMC) such as e.g., such with the polyimide resin as a matrix. Such composite can tolerate long-term service temperature up to 400 °C and may be useful for the components in aerospace [368]. Thermally sprayed coatings on polymers may increase their service temperature and improve their thermal shock resistance [369]. Presently, the low melting point metals as zinc or aluminum are used as bond coat adhering to polymer surface and ceramics are used as top coats for the TBCs on the composite substrate [370]. The failure of such TBC's occurs as vertical cracks through the coating followed by its delamination [371]. To reduce the residual stresses between polymer substrate and ceramic coating the use of ceramic TC having the CTE close to that of the polymer substrate would promote thermal shock resistance [372]. The group around Ivosevic [96,373–375] initiated the studies of FGC on PMC substrates. They used HVOF sprayed graded polyamide/WC-Co coatings to improve adhesion between carbon reinforced PMC substrate and WC-Co top coatings [96]. The bond strength of bond coat was relatively low with the value of 8 MPa. Similar value had the bond strength of coatings arc sprayed with cored wire consisting of low carbon steel skin and Ni–Cr–B–Si filler material on the substrate being graphite fiber reinforced thermo-setting polyimide [376]. Some investigations of sprayed FGC on polymer matrix composites were focused on modification of top layer of composite with metal-polymer mixture [377,378]. Cui et al. [377] used epoxy resin filled with aluminum powder interlayer to deposit aluminum coating with detonation gun on PMC. The bond strength of Al top coat was about 8.6 MPa. Rezzoug et al. [378] sprayed different coatings including e.g., pure epoxy resin layer and its composites with copper, stainless steel and aluminum and reached adhesion varying between 2.7 and 6.5 MPa.

5.2. New Applications of FGC

The number of applications of functionally graded coatings is still growing. In this section only a few examples are briefly described. The development of new materials and new deposition methods enables predicting many new implementation of FGC systems.

Presently, the bond coats of TBC are usually deposited using expensive vacuum plasma spraying (VPS). This spray technique can be replaced by cold spray and by HVOF spraying [379–381]. The emerging technology on this field is cold spraying.

Karaoglanli and Turk [380] tested cold spraying bond coats in the TBC for isothermal oxidation behavior. The authors confirmed the usefulness of cold spraying for bond coat manufacturing. Khanna and Rathod [381] found that bond coat manufactured by cold spraying has satisfactory tribological properties and high oxidation resistance in high temperatures. Go et al. [382] presented cold sprayed coatings using Cr_2AlC powder for TBC bond coat.

Another example of bond coat deposition by cold spraying was a FGC system deposited onto polymer substrate for biomedical applications [383]. The authors describe the bond coat of titanium produced on the biocompatible PEEK substrate. The nanostructured TiO_2 crystallized, as anatase was a top coat.

The new idea of metal-doped HA thermally sprayed coatings was studied to improve antibacterial resistance of bone prostheses, dental implants, and macroporous scaffolds [384]. Sergi et al. [183] produced HA doped with Zn coatings by SPPS method. The tests carried out revealed the coatings bioactivity and their efficiency against some bacteria. The enhanced antibacterial properties of plasma sprayed HA coatings doped with Sr and Zn showed the reduction of cytotoxic effect of Zn^{2+} ions by addition of Sr^{2+} as observed Ullah et al. [385]. Copper can be a useful dopant to the HA improving bactericidal properties sprayed coatings. The characterization of Cu- and Ag-doped HA coatings obtained by APS was carried out by Lyasnikova et al. [386]. The HA with Cu cermet obtained by SSPS technique was characterized by Unabia et al. [184,387]. The improvement of biomedical properties of plasma sprayed HA coatings doped with Mg or with Mg and Sr were found in [388,389]. Another popular dopant of HA coatings is silver. The Ag addition to HA coatings improves bactericidal capacities and decreases the risk of infections after surgery. This type of biomedical coatings were obtained by many thermal spray methods such as vacuum plasma spraying, flame spraying, radio frequency plasma spraying, and suspension plasma spraying [390–394]. The new generation of biomaterials uses magnesium alloys as a substrate on which HA coatings doped with niobium were deposited [395].

To finish, let us have a look on an interesting application of high-pressure cold sprayed alumina composites with aluminum. The coatings were characterized by low thermal conductivity, low solar radiation absorption, comparatively high infrared emittance, and oxidation stability which rendered them useful for application in outer space [396].

6. Conclusions

The paper briefly reviews the application of functionally graded coatings obtained by thermal spray technology. Initially, the conventional thermal spray techniques such as atmospheric plasma spraying (APS) and high velocity oxy-fuel (HVOF) were described. Then new processes such as suspension and solution precursor plasma spraying (SPS and SPPS), and finally low and high pressure cold gas (CGSM) spray methods were shown. Some examples of post spray treatment of coatings used to improve the coatings' properties were described. The solid and liquid feedstock, such as suspension and solution, used in thermal spray technology was shortly discussed. The properties of functionally graded coatings including the methods of characterization were reviewed and some applications of the coatings as thermal barriers, the bio-medical coatings in prostheses, photo-catalytic coatings in water and air treatment, coatings used in printing industry (anilox and corona rolls) were described. Finally, the future possible fields of functional thermal sprayed coatings applications to coat polymer substrates or to use the cheap technology of CGSM instead of more expensive technology of vacuum plasma spraying (VPS) to obtain bond coatings were carefully discussed.

The functionally graded coatings are an important part of thermal spray technology evolution. The FGC enables better association of different materials serving as coating and as substrate. This evolution is carried out on more or less conventional way. The conventional way includes spraying of multi-coatings using mixtures of powders or injecting them separately. The emerging

methods include e.g., the hybrid technologies which use different feedstocks such as e.g., powder and suspensions or suspension and solution.

Author Contributions: For research articles with several authors, a short paragraph specifying their individual contributions must be provided. Conceptualization, L.P. and L.Ł.; writing—original draft preparation, L.Ł., L.P., M.W., P.S., A.M., S.K. writing—review and editing, L.Ł., L.P. All authors have read and agreed to the published version of the manuscript.

Funding: This research received no external funding.

Conflicts of Interest: The authors declare no conflict of interest.

Abbreviations

Abbreviations	
7YSZ or 8YSZ	ZrO_2 + 7 or 8 wt.% Y_2O_3
APS	atmospheric plasma spraying
ASTM	American Society of Testing Materials
BC	bond coat
BSE	back scattered electrons
CGSM	cold gas spray method
CTE	coefficient of thermal expansion
CVD	chemical vapor deposition
CYSZ	ceria and yttria stabilized zirconia
FGC	functionally graded coatings
FSP	friction stir processing
HA	hydroxyapatite
HCPD	high-pressure cold spraying
HIP	hot isostatic pressing
HVAF	high velocity air fuel
HVOF	high velocity oxy- fuel
HVSFS	high velocity suspension flame spraying
IIT	instrumented indentation test
ISO	International Standard Organization
LPCS	low pressure cold spraying
MMC	metal matrix composites
PEEK	polyether ether ketone
PMC	polymer matrix composite
PVD	physical vapor deposition
SEM	scanning electron microscope
SPPS	solution precursor plasma spraying
SBF	simulated body fluid
SPS	suspension plasma spraying
TAT	tensile adhesion test
TBC	thermal barrier coating
TGO	thermally grown oxide
TC	top coat
TS	thermal spraying
UV	ultraviolet
YSZ	yttria stabilized zirconia
Symbols	
Ev	evaporated gas
GI_c	energy release rate
HV	Vickers microhardness
KI_c	fracture toughness
L	liquid
S	solid
T_m	melting point

References

1. Pawłowski, L. *The Science and Engineering of Thermal Spray Coatings*, 2nd ed.; Wiley and Sons: Chichester, UK, 2008.
2. Zhang, T.; Gawne, D.T.; Bao, Y. The influence of process parameters on the degradation of thermally sprayed polymer coatings. *Surf. Coat. Technol.* **1997**, *96*, 337–344. [CrossRef]
3. Leivo, E.; Wilenius, T.; Kinos, T.; Vuoristo, P.; Mäntylä, T. Properties of thermally sprayed fluoropolymer PVDF, ECTFE, PFA and FEP coatings. *Prog. Org. Coat.* **2004**, *49*, 69–73. [CrossRef]
4. Website of Research and Markets. Thermal Spray Coating Market by Material, Process and End-Use Industry: Opportunity Analysis and Industry Forecast, 2019–2026. Available online: https://www.researchandmarkets.com/reports/5031511/thermal-spray-coating-market-by-material-process?utm_source=MC&utm_medium=Email&utm_code=mzr1whfdt&utm_ss=29&utm_campaign=1399699+-+Thermal+Spray+Coating+Market+(2019-2026)&utm_exec=adke277mtd (accessed on 24 June 2020).
5. Giannini, G.; Ducati, A. Plasma Stream Apparatus and Method. U.S. Patent 2 922 869, 31 January 1960.
6. Gage, R.M.; Nestor, D.M.; Yenni, Y.M. Collimated Electric Arc Powder Deposition Process. U.S. Patent 3 016 447, 12 December 1962.
7. Heimann, R.B. *Plasma Spray Coatings, Principles and Applications*, 2nd ed.; Wiley: Oxford, UK, 2008.
8. Pawlowski, L. Finely grained nanometric and submicrometric coatings by thermal spraying: A review. *Surf. Coat. Technol.* **2008**, *202*, 4318–4328. [CrossRef]
9. Pateyron, B.; Elchinger, M.F.; Delluc, G.; Fauchais, P. Thermodynamic and transport properties of Ar-H_2 and Ar-He plasma gases used for spraying at atmospheric pressure. I: Properties of the mixtures. *Plasma Chem. Plasma Process.* **1992**, *12*, 421–448. [CrossRef]
10. Fauchais, P.L.; Heberlein, J.V.R.; Boulos, M.I. *Thermal Spray Fundamentals, from Powder to Part*; Springer: Berlin/Heidelberg, Germany, 2014.
11. Thirumalaikumarasamy, D.; Shanmugam, K.; Balasubramanian, V. Effect of atmospheric plasma spraying parameters on porosity level of alumina coatings. *Surf. Eng.* **2012**, *28*, 759–766. [CrossRef]
12. Rico, A.; Salazar, A.; Escobar, M.E.; Rodriguez, J.; Poza, P. Optimization of atmospheric low-power plasma spraying process parameters of Al_2O_3-50 wt.% Cr_2O_3 coatings. *Surf. Coat. Technol.* **2018**, *354*, 281–296. [CrossRef]
13. Łatka, L.; Michalak, M.; Jonda, E. Atmospheric plasma spraying of Al_2O_3 + 13% TiO_2 coatings using external and internal injection system. *Adv. Mater. Sci.* **2019**, *19*, 5–17. [CrossRef]
14. Pawłowski, L. Thermal spray coatings. In *Encyclopedia of Composites*; Nicolais, L., Borzacchiello, A., Eds.; Wiley and Sons: Chichester, UK, 2012; pp. 3014–3034.
15. Toma, F.L.; Scheitz, S.; Berger, L.-M.; Sauchuk, V.; Kusnezoff, M.; Thiele, S. Comparative study of the electrical properties and characteristics of thermally sprayed alumina and spinal coatings. *J. Therm. Spray Technol.* **2011**, *20*, 195–204. [CrossRef]
16. Ahn, H.S.; Kwon, O.K. Tribological behavior of plasma-sprayed chromium oxide coating. *Wear* **1999**, *225–229*, 814–824. [CrossRef]
17. Łatka, L.; Szala, M.; Michalak, M.; Pałka, T. Impact of atmospheric plasma spray parameters on cavitation erosion resistance of Al_2O_3-13% TiO_2 coatings. *Acta Phys. Pol. A* **2019**, *136*, 342–347. [CrossRef]
18. Zeng, Y.; Lee, S.W.; Ding, C. Study on plasma sprayed boron carbide coating. *J. Therm. Spray Technol.* **2002**, *11*, 129–133. [CrossRef]
19. Li, H.J.; Fu, Q.G.; Yao, D.J.; Wang, Y.J.; Ma, C.; Wei, J.F.; Han, Z.H. Microstructures and ablation resistance of ZrC coating for SiC-coated carbon/carbon composites prepared by supersonic plasma spraying. *J. Therm. Spray Technol.* **2011**, *20*, 1286–1291.
20. Ageorges, H.; Ctibor, P.; Medarhri, Z.; Touimi, S.; Fauchais, P. Influence of the metallic matrix ratio on the wear resistance (dry and slurry abrasion) of plasma sprayed cermet (chromia/stainless steel) coatings. *Surf. Coat. Technol.* **2006**, *201*, 2006–2011. [CrossRef]
21. Basak, A.K.; Achanta, S.; Celis, J.P.; Vardavoulias, M.; Matteazzi, P. Structure and mechanical properties of plasma sprayed nanostructured alumina and FeCuAl-alumina cermet coatings. *Surf. Coat. Technol.* **2008**, *202*, 2368–2373. [CrossRef]
22. Hashemi, S.M.; Enayati, M.H.; Fathi, M.H. Plasma spray coatings of Ni-Al-SiC composite. *J. Therm. Spray Technol.* **2009**, *18*, 284–291. [CrossRef]
23. Michalak, M.; Łatka, L.; Sokołowski, P.; Niemiec, A.; Ambroziak, A. The microstructure and selected mechanical properties of Al_2O_3 + 13 wt.% TiO_2 plasma sprayed coatings. *Coatings* **2020**, *10*, 173. [CrossRef]

24. Fauchais, P.; Montavon, G.; Bertrand, G. From powders to thermally sprayed coatings. *J. Therm. Spray Technol.* **2009**, *19*, 56–80. [CrossRef]
25. Kopp, G.; Baumann, I.; Vogli, E.; Tillmann, W.; Weihs, C. Desirability-based multi-criteria optimization of HVOF spray experiments. In *Classification as a Tool for Research*; Locarek-Junge, H., Weihs, C., Eds.; Springer: Berlin/Heidelberg, Germany, 2010; pp. 811–818.
26. Gitzhofer, F.; Bouyer, E.; Boulos, M.I. Suspension Plasma Spray. U.S. Patent US5609921 A, 26 August 1997.
27. Sokołowski, P.; Pawłowski, L. Review of recent studies on suspension plasma sprayed ZrO_2 coatings. In *Advances in Materials Science Research*; Wythers, M.C., Ed.; Nova: New York, NY, USA, 2016; Volume 26, pp. 137–181.
28. Ganvir, A.; Curry, N.; Markocsan, N.; Nylén, P.; Toma, F.-L. Comparative study of suspension plasma sprayed and suspension high velocity oxy-fuel sprayed YSZ thermal barrier coatings. *Surf. Coat. Technol.* **2015**, *268*, 70–76. [CrossRef]
29. Berghaus, J.O.; Marple, B.; Moreau, C. Suspension plasma spraying of nanostructured WC-12Co coatings. *J. Therm. Spray Technol.* **2006**, *15*, 676–681. [CrossRef]
30. Sokołowski, P.; Nylen, P.; Musalek, R.; Łatka, L.; Kozerski, S.; Dietrich, D.; Lampke, T.; Pawłowski, L. The microstructural studies of suspension plasma sprayed zirconia coatings with the use of high-energy plasma torches. *Surf. Coat. Technol.* **2017**, *318*, 250–261. [CrossRef]
31. Bacciochini, A.; Montavon, G.; Ilavsky, J.; Denoirjean, A.; Fauchais, P. Porous architecture of SPS thick YSZ coatings structured at the nanometer scale (~50 nm). *J. Therm. Spray Technol.* **2010**, *19*, 198–206. [CrossRef]
32. Klement, U.; Ekberg, J.; Creci, S.; Kelly, S.T. Porosity measurements in suspension plasma sprayed YSZ coatings using NMR cryoporometry and X-ray microscopy. *J. Coat. Technol. Res.* **2018**, *15*, 753–757. [CrossRef]
33. Curry, N.; VanEvery, K.; Snyder, T.; Susnjar, J.; Björklund, S. Performance testing of suspension plasma sprayed thermal barrier coatings produced with varied suspension parameters. *Coatings* **2015**, *5*, 338–356. [CrossRef]
34. Znamirowski, Z.; Posadowski, W.; Pawłowski, L.; Cattini, A.; Łatka, L. Electron emission from the zirconium coated suspension plasma sprayed bioglass. *Surf. Coat. Technol.* **2015**, *268*, 63–69. [CrossRef]
35. Sokolowski, P. Properties of Suspension Plasma Sprayed Zirconia Coatings Using Different Plasma Torches. Ph.D. Thesis, University of Limoges, Limoges, France, 2016.
36. Podlesak, H.; Pawlowski, L.; d'Haese, R.; Laureyns, J.; Lampke, T.; Bellayer, S. Advanced microstructural study of suspension plasma sprayed hydroxyapatite coatings. *J. Therm. Spray Technol.* **2010**, *19*, 657–664. [CrossRef]
37. Kozerski, S.; Pawłowski, L.; Jaworski, R.; Roudet, F.; Petit, F. Two zones microstructure of suspension plasma sprayed hydroxyapatite coatings. *Surf. Coat. Technol.* **2010**, *204*, 1380–1387. [CrossRef]
38. Shahien, M.; Suzuki, M.; Tsutai, Y. Controlling the coating microstructure on axial suspension plasma spray process. *Surf. Coat. Technol.* **2018**, *356*, 96–107. [CrossRef]
39. Fauchais, F.; Vardelle, M.; Coudert, J.F.; Vardelle, A.; Delbos, C.; Fazilleau, J. Thermal plasma deposition from thick to thin coatings and from micro- to nanostructure. *Pure Appl. Chem.* **2005**, *77*, 475–485. [CrossRef]
40. Watanabe, Y.; Sato, H.; Miura-Fujiwara, E. Functionally graded metallic biomaterials. In *Advances in Metallic Biomaterials: Processing and Applications*; Niinomi, M., Narushima, T., Nakai, M., Eds.; Springer: Berlin/Heidelberg, Germany, 2015; pp. 181–209.
41. Cattini, A.; Bellucci, D.; Sola, A.; Pawłowski, L.; Cannillo, V. Suspension plasma spraying of optimized functionally graded coatings of bioactive glass/hydroxyapatite. *Surf. Coat. Technol.* **2013**, *236*, 118–126. [CrossRef]
42. Cattini, A.; Bellucci, D.; Sola, A.; Pawłowski, L.; Cannillo, V. Microstructural design of functionally graded coatings composed of suspension plasma sprayed hydroxyapatite and bioactive glass. *J. Biomed. Mater. Res. B Appl. Biomater.* **2014**, *102*, 551–560. [CrossRef]
43. Tomaszek, R.; Pawłowski, L.; Gengembre, L.; Laureyns, J.; Le Maguer, A. Microstructure of suspension plasma sprayed multilayer coatings of hydroxyapatite and titanium oxide. *Surf. Coat. Technol.* **2007**, *201*, 7432–7440. [CrossRef]
44. Björklund, S.; Goel, S.; Joshi, S.V. Function-dependent coating architectures by hybrid powder-suspension plasma spraying: Injector design, processing and concept validation. *Mater. Des.* **2018**, *142*, 56–65. [CrossRef]
45. Wang, C.; Wang, Y.; Fan, S.; You, Y.; Wang, L.; Yang, C.; Sun, X.; Li, X. Optimized functionally graded $La_2Zr_2O_7$/8YSZ thermal barrier coatings fabricated by suspension plasma spraying. *J. Alloys Compd.* **2015**, *649*, 1182–1190. [CrossRef]
46. Karthikeyan, J.; Berndt, C.C.; Tikkanen, J.; Wang, J.Y.; King, A.H.; Herman, H. Preparation of nanophase materials by thermal spray processing of liquid precursors. *Nanostruct. Mater.* **1997**, *9*, 137–140. [CrossRef]

47. Karthikeyan, J.; Berndt, C.C.; Tikkanen, J.; Wang, J.Y.; King, A.H.; Herman, H. Nanomaterial powders and deposits prepared by flame spray processing of liquid precursors. *Nanostruct. Mater.* **1997**, *8*, 61–74. [CrossRef]
48. Tikkanen, J.; Gross, K.A.; Berndt, C.C.; Pitkanen, V.; Keskinen, J.; Raghu, B.; Rajala, M.; Karthikeyan, J. Characteristic of the liquid flame spray process. *Surf. Coat. Technol.* **1997**, *90*, 210–216. [CrossRef]
49. Karthikeyan, J.; Berndt, C.C.; Tikkanen, J.; Reddy, S.; Herman, H. Plasma spray synthesis of nanomaterial powders and deposits. *Mater. Sci. Eng. A* **1997**, *238*, 275–286. [CrossRef]
50. Karthikeyan, J.; Berndt, C.C.; Reddy, S.; Wang, J.Y.; King, A.H.; Herman, H. Nanomaterial deposits formed by DC plasma spraying of liquid feedstocks. *J. Am. Ceram. Soc.* **1998**, *81*, 121–128. [CrossRef]
51. Pawłowski, L. Application of solution precursor spray techniques to obtain ceramic films and coatings. In *Future Development of Thermal Spray Coatings: Types, Designs, Manufacture and Applications*; Espallargas, N., Ed.; Elsevier Ltd.: Oxford, UK, 2015; pp. 123–141.
52. Padture, N.P.; Schlichting, K.W.; Bhatia, T.; Ozturk, A.; Cetegen, B.; Jordan, E.H.; Gell, M.; Jiang, S.; Xiao, T.D.; Strutt, P.R.; et al. Towards durable thermal barrier coatings with novel microstructures deposited by solution precursor plasma spraying. *Acta Mater.* **2001**, *49*, 2251–2257. [CrossRef]
53. Parukuttyamma, S.D.; Margolis, J.; Liu, H.; Grey, C.P.; Sampath, S.; Herman, H.; Parise, J.B. Yttrium aluminum garnet (YAG) films through a precursor plasma spraying technique. *J. Am. Ceram. Soc.* **2001**, *84*, 1906–1908. [CrossRef]
54. Govindarajan, S.; Dusane, R.O.; Joshi, S.V. In situ particles generation and splat formation during solution precursor plasma spraying of yttria stabilized zirconia coatings. *J. Am. Ceram. Soc.* **2011**, *94*, 4191–4199. [CrossRef]
55. Yang, T.; Ma, W.; Meng, X.; Huang, W.; Bai, Y.; Dong, H. Deposition characteristics of CeO_2-Gd_2O_3 co-stabilized zirconia (CGZ) coating prepared by solution precursor plasma spray. *Surf. Coat. Technol.* **2020**, *381*, 125114. [CrossRef]
56. Metcalfe, C.; Lay-Grindler, E.; Kesler, O. Characterization of Ni–YSZ anodes for solid oxide fuel cells fabricated by solution precursor plasma spraying with axial feedstock injection. *J. Power Sources* **2014**, *247*, 831–839. [CrossRef]
57. Shri Prakash, B.; Senthil Kumar, S.; Aruna, S.T. Microstructure and performance of LSM/YSZ based solid oxide fuel cell cathodes fabricated from solution combustion co-synthesized powders and by solution precursor plasma spraying. *Surf. Coat. Technol.* **2017**, *310*, 25–32. [CrossRef]
58. Candidato, R.T., Jr.; Sokołowski, P.; Pawłowski, L.; Lecomte-Nana, G.; Constantinescu, C.; Denoirjean, A. Development of hydroxyapatite coatings by solution precursor plasma spray process and their microstructural characterization. *Surf. Coat. Technol.* **2017**, *318*, 39–49. [CrossRef]
59. Canas, E.; Orts, M.J.; Boccaccini, A.R.; Sanchez, E. Microstructural and in vitro characterization of 45S5 bioactive glass coatings deposited by solution precursor plasma spraying (SPPS). *Surf. Coat. Technol.* **2019**, *371*, 151–160. [CrossRef]
60. Dom, E.; Sivakumar, G.; Hebalkar, N.Y.; Joshi, S.V.; Borse, P.H. Deposition of nanostructured photocatalytic zinc ferrite films using solution precursor plasma spraying. *Mater. Res. Bull.* **2012**, *47*, 562–570. [CrossRef]
61. Yu, Z.; Moussa, H.; Liu, M.; Schneider, R.; Wang, W.; Moliere, M.; Liao, H. Development of photocatalytically active heterostructured MnO/ZnO and CuO/ZnO films via solution precursor plasma spray process. *Surf. Coat. Technol.* **2019**, *371*, 107–116. [CrossRef]
62. Zhang, C.; Wang, J.; Geng, X. Tungsten oxide coatings deposited by plasma spray using powder and solution precursor for detection of nitrogen dioxide gas. *J. Alloys Compd.* **2016**, *668*, 128–136. [CrossRef]
63. Yu, Z.X.; Ma, Y.Z.; Zhao, Y.L.; Huang, J.B.; Wang, W.Z.; Moliere, M.; Liao, H.L. Effect of precursor solutions on ZnO film via solution precursor plasma spray and corresponding gas sensing performances. *Appl. Surf. Sci.* **2017**, *412*, 683–689. [CrossRef]
64. Darthout, E.; Laduye, G.; Gitzhofer, F. Processing parameter effects and thermal properties of $Y_2Si_2O_7$ nanostructured environmental barrier coatings synthesized by solution precursor induction plasma spraying. *J. Therm. Spray Technol.* **2016**, *25*, 1264–1279. [CrossRef]
65. Wang, X.; Li, X.; Li, C.; Tian, L.; Yang, G. Microstructure and electrochemical behavior of $La_{0.8}Sr_{0.2}MnO_3$ deposited by solution precursor plasma spraying. *Rare Met. Mater. Eng.* **2011**, *40*, 1881–1886.
66. Mavier, F.; Zoubian, F.; Bienia, M.; Coudert, J.F.; Lejeune, M.; Rat, V.; Andre, P. Plasma spraying of solution precursor in pulsed mode: In-flight phenomena and coating deposition. *Plasma Chem. Plasma Process.* **2018**, *38*, 657–682. [CrossRef]
67. Canas, E.; Orts, M.J.; Boccaccini, A.R.; Sanchez, E. Solution Precursor Plasma Spraying (SPPS): A novel and simple process to obtain bioactive glass coatings. *Mater. Lett.* **2018**, *223*, 198–202. [CrossRef]

68. Basu, S.; Jordan, E.H.; Cetegen, B.M. Fluid mechanics and heat transfer of liquid precursor droplets injected into high-temperature plasmas. *J. Therm. Spray Technol.* **2008**, *17*, 60–72. [CrossRef]
69. Golozar, M.; Chien, K.; Lian, K.; Coyle, T.W. Pseudo-capacitors: SPPS deposition and electrochemical analysis of α-MoO_3 and Mo_2N coatings. *J. Therm. Spray Technol.* **2013**, *22*, 710–722. [CrossRef]
70. Jordan, E.H.; Jiang, C.; Gell, M. The solution precursor plasma spray (SPPS) process: A review with energy considerations. *J. Therm. Spray Technol.* **2015**, *24*, 1153–1165. [CrossRef]
71. Fauchais, P.; Rat, V.; Coudert, J.F.; Etchart-Salas, R.; Montavon, G. Operating parameters for suspension and solution plasma-spray coatings. *Surf. Coat. Technol.* **2008**, *202*, 4309–4317. [CrossRef]
72. Sanpo, N. *Solution Precursor Plasma Spray System*; Springer International Publishing: Berlin/Heidelberg, Germany, 2014.
73. Wang, R.; Duan, J.; Ye, F. Effect of spraying parameters on the crystallinity and microstructure of solution precursor plasma sprayed coatings. *J. Alloys Compd.* **2018**, *766*, 886–893. [CrossRef]
74. Khan, M.; Hu, N.; Zhenhua, L.; Wang, Y.; Yi, Z. Influence of solution-precursor plasma spray (SPPS) processing parameters on the mechanical and thermodynamic properties of 8 YSZ. *Ceram. Int.* **2018**, *44*, 7794–7798. [CrossRef]
75. Pawłowski, L. Suspension and solution thermal spray coatings. *Surf. Coat. Technol.* **2009**, *203*, 2807–2829. [CrossRef]
76. Xiong, H.; Sun, W. Investigation of droplet atomization and evaporation in solution precursor plasma spray coating. *Coatings* **2017**, *7*, 207. [CrossRef]
77. Tobon Valencia, V.; Pawłowski, L.; Lecomte-Nana, G.; Constantinescu, C.; Pateyron, B. Preliminary analysis of physical and chemical phenomena occurring in droplet at solution precursor plasma spraying of zirconia coatings. *Surf. Coat. Technol.* **2020**, *397*, 126059. [CrossRef]
78. Joulia, A.; Bolelli, G.; Gualtieri, E.; Lusvarghi, L.; Valeri, S.; Vardelle, M.; Rossignol, S.; Vardelle, A. Comparing the deposition mechanisms in suspension plasma spray (SPS) and solution precursor plasma spray (SPPS) deposition of yttria-stabilised zirconia (YSZ). *J. Eur. Ceram. Soc.* **2014**, *34*, 3925–3940. [CrossRef]
79. Yu, Z.; Moussa, H.; Liu, M.; Schneider, R.; Moliere, M.; Liao, H. Solution precursor plasma spray process as an alternative rapid one-step route for the development of hierarchical ZnO films for improved photocatalytic degradation. *Ceram. Int.* **2018**, *44*, 2085–2092. [CrossRef]
80. Fauchais, P.; Vardelle, A.; Vardelle, M. Thermally sprayed nanoceramic and nanocomposite coatings. In *Handbook of Nanoceramic and Nanocomposite Coatings and Materials*; Makhlouf, A.S.H., Scharnweber, D., Eds.; Elsevier: Oxford, UK, 2015.
81. Joshi, S.V.; Sivakumar, G. Hybrid processing with powders and solutions: A novel approach to deposit composite coatings. *J. Therm. Spray Technol.* **2015**, *24*, 1166–1186. [CrossRef]
82. Hou, H.; Veilleux, J.; Gitzhofer, F.; Wang, Q.; Iiu, Y. Hybrid suspension/solution precursor plasma spraying of a complex $Ba(Mg_{1/3}Ta_{2/3})O_3$ perovskite: Effects of processing parameters and precursor chemistry on phase formation and decomposition. *J. Therm. Spray Technol.* **2019**, *28*, 12–26. [CrossRef]
83. Shan, Y.; Coyle, T.W.; Mostaghimi, J. 3D modeling of transport phenomena and the injection of the solution droplets in the solution precursor plasma spraying. *J. Therm. Spray Technol.* **2007**, *16*, 736–743. [CrossRef]
84. Carpio, P.; Pawłowski, L.; Pateyron, B. Numerical investigation of influence of precursors on transport properties of the jets used in solution precursor plasma spraying. *Surf. Coat. Technol.* **2019**, *371*, 131–135. [CrossRef]
85. Fan, W.; Bai, Y. Review of suspension and solution precursor plasma sprayed thermal barrier coatings. *Ceram. Int.* **2016**, *42*, 14299–14312. [CrossRef]
86. Xie, L.; Ma, X.; Jordan, E.H.; Padture, N.P.; Xiao, D.T.; Gell, M. Deposition mechanisms of thermal barrier coatings in the solution precursor plasma spray process. *Surf. Coat. Technol.* **2004**, *177–178*, 103–107. [CrossRef]
87. Xu, P.; Coyle, T.W.; Pershin, L.; Mostaghimi, J. Fabrication of superhydrophobic ceramic coatings via solution precursor plasma spray under atmospheric and low-pressure conditions. *J. Therm. Spray Technol.* **2019**, *28*, 242–254. [CrossRef]
88. Planche, M.P.; Liao, H.; Normand, B.; Coddet, C. Relationships between NiCrBSi particle characteristics and corresponding coating properties using different thermal spraying processes. *Surf. Coat. Technol.* **2005**, *200*, 2465–2473. [CrossRef]
89. Hasan, M.; Stokes, J.; Looney, L.; Hashmi, M.S.J. Effect of spray parameters on residual stress build-up of HVOF sprayed aluminium/tool-steel functionally graded coatings. *Surf. Coat. Technol.* **2008**, *202*, 4006–4010. [CrossRef]
90. Kamara, A.M.; Davey, K. Simplified models for residual stress prediction in thermally sprayed coatings. *Proc. Inst. Mech. Eng. C.J. Mech. Eng. Sci.* **2008**, *222*, 2053–2068. [CrossRef]

91. Prchlik, L.; Sampath, S.; Gutleber, J.; Bancke, G.; Ruff, A.W. Friction and wear properties of WC-Co and Mo-Mo2C based functionally graded materials. *Wear* **2001**, *249*, 1103–1115. [CrossRef]
92. Mamun, K.A.; Stokes, J. Development of a semi-automated dual feed unit to produce FGM coatings using the HVOF thermal spray process. *S. Pac. J. Nat. A Sci.* **2014**, *32*, 18. [CrossRef]
93. Bolelli, G.; Cannillo, V.; Lusvarghi, L.; Rosa, R.; Valarezo, A.; Choi, W.B.; Dey, R.; Weyant, C.; Sampath, S. Functionally graded WC–Co/NiAl HVOF coatings for damage tolerance, wear and corrosion protection. *Surf. Coat. Technol.* **2012**, *206*, 2585–2601. [CrossRef]
94. Hasan, M.; Stokes, J.; Looney, L.; Hashmi, M.S.J. Design and optimisation of a multi-powder feed system for the HVOF deposition process. *Surf. Coat. Technol.* **2008**, *202*, 3215–3220. [CrossRef]
95. Zimmermann, J.R.A.; Schab, J.C.; Stankowski, A.; Grasso, P.D.; Olliges, S.; Leyens, C. Modular coating for flexible gas turbine operation. *J. Therm. Spray Technol.* **2016**, *25*, 273–281. [CrossRef]
96. Ivosevic, M.; Knight, R.; Kalidindi, S.R.; Palmese, G.R.; Sutter, J.K. Adhesive/cohesive properties of thermally sprayed functionally graded coatings for polymer matrix composites. *J. Therm. Spray Technol.* **2005**, *14*, 45–51. [CrossRef]
97. Saaedi, J.; Coyle, T.W.; Arabi, H.; Mirdamadi, S.; Mostaghimi, J. Effects of HVOF process parameters on the properties of Ni-Cr coatings. *J. Therm. Spray Technol.* **2010**, *19*, 521–530. [CrossRef]
98. Yunanto, A.G. Influence of process parameters on HVOF coating quality: A review. *Ann. Conf. Manag. Inform. Technol.* **2016**, *3*, 166–170. [CrossRef]
99. Hasan, M.; Stokes, J.; Looney, L.; Hashmi, M.S.J. Deposition and characterization of HVOF thermal sprayed functionally graded coatings deposited onto a lightweight material. *J. Mater. Eng. Perform.* **2009**, *18*, 66–69. [CrossRef]
100. Schulz, U.; Peters, M.; Bach, F.-W.; Tegeder, G. Graded coatings for thermal, wear and corrosion barriers. *Mater. Sci. Eng. A* **2003**, *362*, 61–80. [CrossRef]
101. Henao, J.; Cruz-Bautista, M.; Hincapie-Bedoya, J.; Ortega-Bautista, B.; Corona-Castuera, J.; Giraldo-Betancur, A.L.; Espinoza-Arbelaez, D.G.; Alvarado-Orozco, J.M.; Clavijo-Mejia, G.A.; Trapaga-Martinez, L.G.; et al. HVOF hydroxyapatite/titania graded coatings: Microstructural, mechanical and in vitro characterization. *J. Therm. Spray Technol.* **2018**, *27*, 1302–1321. [CrossRef]
102. Yao, H.L.; Wang, H.T.; Bai, X.B.; Ji, G.C.; Chen, Q.Y. Improvement in mechanical properties of nano-structured HA/TiO_2 multilayer coatings deposited by high velocity suspension flame spraying (HVSFS). *Surf. Coat. Technol.* **2018**, *342*, 94–104. [CrossRef]
103. Borchers, C.; Gärtner, F.; Stoltenhoff, T.; Assadi, H.; Kreye, H. Microstructural and microscopic properties of cold sprayed copper coatings. *J. Appl. Phys.* **2003**, *93*, 10064–10070. [CrossRef]
104. Maev, R.; Leshchynsky, V. Air gas dynamic spraying of powder mixtures: Theory and applications. *J. Therm. Spray Technol.* **2006**, *15*, 198–205. [CrossRef]
105. Papyrin, A. *Cold Spray Technology*; Elsevier: Oxford, UK, 2007.
106. Stoltenhoff, T.; Kreye, H.; Richter, H. An analysis of the cold spray process and its coatings. *J. Therm. Spray Technol.* **2001**, *11*, 542–550. [CrossRef]
107. Gujicic, M.; Zhao, C.; Tong, C.; DeRosset, W.; Helfricht, D. Analysis of the impact velocity of powder particels in the cold-gas dynamic-spraying process. *Mat. Sci. Eng. A* **2004**, *368*, 222–230. [CrossRef]
108. Van Steenkiste, T.H.; Smith, J.R.; Teets, R.E.; Moleski, J.J.; Gorkiewicz, D.W.; Tison, R.P.; Marantz, D.R.; Kowalsky, K.A.; Riggs, W.L.; Zajchowski, P.H.; et al. Kinetic spray coatings. *Surf. Coat. Technol.* **1999**, *111*, 62–71. [CrossRef]
109. Sobolev, V.; Guilemany, J.; Nutting, J. *High Velocity Oxy-Fuel Spraying, Theory, Structure-Property Relationship and Applications*; Money Publishing: London, UK, 2004.
110. Zou, Y.; Qin, W.; Irissou, E.; Legoux, J.-G.; Yue, S.; Szpunar, J. Dynamic recrystallization in the particle/particle interfacial region of cold-sprayed nickel coating: Electron backscatter diffraction characterization. *Scripta Mater.* **2009**, *61*, 899–902. [CrossRef]
111. Gärtner, F.; Schmidt, T.; Stoltenhoff, T.; Kreye, H. Recent developments and potential applications of cold spraying. *Adv. Eng. Mater.* **2006**, *8*, 611–618. [CrossRef]
112. Assadi, H.; Kreye, H.; Gärtner, F.; Klassen, T. Cold spraying—A materials perspective. *Acta Mater.* **2016**, *116*, 382–407. [CrossRef]
113. Rokni, M.R.; Nutt, S.R.; Widener, C.A.; Champagne, V.K.; Hrabe, R.H. Review of relationship between particle deformation, coating microstructure, and properties in high-pressure cold spray. *J. Therm. Spray. Technol.* **2017**, *26*, 1308–1355. [CrossRef]
114. Yin, S.; Cavaliere, P.; Aldwell, B.; Jenkins, R.; Liao, H.; Li, W.; Lupoi, R. Cold spray additive manufacturing and repair: Fundamentals and applications. *Add. Manuf.* **2018**, *21*, 628–650. [CrossRef]

115. Grigoriev, S.; Okunkova, A.; Sova, A.; Bertrand, P.; Smurov, I. Cold spraying: From process fundamentals towards advanced applications. *Surf. Coat. Technol.* **2015**, *268*, 77–84. [CrossRef]
116. Koivuluoto, H.; Honkanen, M.; Vuoristo, P. Cold-sprayed copper and tantalum coatings—Detailed FESEM and TEM analysis. *Surf. Coat. Technol.* **2010**, *204*, 2353–2361. [CrossRef]
117. Winnicki, M.; Małachowska, A.; Ambroziak, A. Taguchi optimization of the thickness of a coating deposited by LPCS. *Arch. Civ. Mech. Eng.* **2014**, *14*, 561–568. [CrossRef]
118. Wang, Q.; Spencer, K.; Birbilis, N.; Zhang, M.-X. The influence of ceramic particles on bond strength of cold spray composite coatings on AZ91 alloy substrate. *Surf. Coat. Technol.* **2010**, *205*, 50–56. [CrossRef]
119. Winnicki, M.; Małachowska, A.; Rutkowska-Gorczyca, M.; Sokołowski, P.; Ambroziak, A.; Pawłowski, L. Characterization of cermet coatings deposited by low-pressure cold spraying. *Surf. Coat. Technol.* **2015**, *268*, 108–114. [CrossRef]
120. Koivuluoto, H.; Vuoristo, P. Effect of powder type and composition on structure and mechanical properties of Cu + Al_2O_3 coatings prepared by using low-pressure cold spray process. *J. Therm. Spray Technol.* **2010**, *19*, 1081–1092. [CrossRef]
121. Koivuluoto, H.; Lagerbom, J.; Kylmalahti, M.; Vuoristo, P. Microstructure and mechanical properties of Low-Pressure Cold-Sprayed (LPCS) coatings. *J. Therm. Spray Technol.* **2008**, *17*, 721–727. [CrossRef]
122. Winnicki, M.; Małachowska, A.; Baszczuk, A.; Rutkowska-Gorczyca, M.; Kukla, D.; Lachowicz, M.; Ambroziak, A. Corrosion protection and electrical conductivity of copper coatings deposited by low-pressure cold spraying. *Surf. Coat. Technol.* **2017**, *318*, 90–98. [CrossRef]
123. Winnicki, M.; Baszczuk, A.; Rutkowska-Gorczyca, M.; Małachowska, A.; Ambroziak, A. Corrosion resistance of tin coatings deposited by cold spraying. *Surf. Eng.* **2016**, *32*, 691–700. [CrossRef]
124. Peat, T.; Galloway, A.; Toumpis, A.; McNutt, P.; Iqbal, N. The erosion performance of particle reinforced metal matrix composite coatings produced by co-deposition cold gas dynamic spraying. *Appl. Surf. Sci.* **2017**, *396*, 1623–1634. [CrossRef]
125. Guillem-Marti, J.; Cinca, N.; Punset, M.; Cano, I.G.; Gil, F.J.; Guilemany, J.M.; Dosta, S. Porous titanium-hydroxyapatite composite coating obtained on titanium by cold gas spray with high bond strength for biomedical applications. *Colloid Surf. B* **2019**, *180*, 245–253. [CrossRef]
126. Winnicki, M.; Małachowska, A.; Piwowarczyk, T.; Rutkowska-Gorczyca, M.; Ambroziak, A. The bond strength of Al + Al_2O_3 cermet coatings deposited by low-pressure cold spraying. *Arch. Civ. Mech. Eng.* **2016**, *16*, 743–752. [CrossRef]
127. Luo, X.T.; Yang, G.J.; Li, C.J. Preparation and characterization of cBNp/NiCrAl nanostructured composite powders by a step-fashion mechanical alloying process. *Powder Technol.* **2012**, *217*, 591–598. [CrossRef]
128. Luo, X.T.; Yang, G.J.; Li, C.J. Multiple strengthening mechanisms of cold-sprayed cBNp/NiCrAl composite coating. *Surf. Coat. Technol.* **2011**, *205*, 4808–4813. [CrossRef]
129. Kumar, M.; Singh, H.; Singh, N. Effect of increase in nano-particle addition on mechanical and microstructural behaviour of HVOF and cold-spray Ni-20Cr coatings on boiler steels. *Mater. Today Proc.* **2020**, *21*, 2035–2042. [CrossRef]
130. Feng, C.; Guipont, V.; Jeandin, M.; Amsellem, O.; Pauchet, F.; Saenger, R.; Bucher, S.; Iac, C. B_4C/Ni composite coatings prepared by cold spray of blended or CVD-coated powders. *J. Therm. Spray Technol.* **2012**, *21*, 561–570. [CrossRef]
131. Yin, S.; Cizek, J.; Chen, C.; Jenkins, R.; O'Donnell, G.; Lupoi, R. Metallurgical bonding between metal matrix and core-shelled reinforcements in cold sprayed composite coating. *Scr. Mater.* **2020**, *177*, 49–53. [CrossRef]
132. Davis, J.R. *Handbook of Thermal Spray Technology*; ASM International: Materials Park, OH, Canada, 2004.
133. Tekkaya, A.E.; Kleiner, M.; Biermann, D.; Hiegemann, L.; Rausch, S.; Franzen, V.; Kwiatkowski, L.; Kersting, P. Friction analysis of thermally sprayed coatings finished by ball burnishing and grinding. *Prod. Eng. Res. Devel.* **2013**, *7*, 601–610. [CrossRef]
134. Zamani, P.; Valefi, Z.; Mirjani, M. Effect of grinding and lubricating post-treatment on wear performance of plasma sprayed Cr_2O_3–Al_2O_3 composite coatings. *Surf. Interfaces* **2019**, *16*, 206–214. [CrossRef]
135. Malkin, S.; Guo, C. *Grinding Technology: Theory and Applications of Machining with Abrasives*; Industrial Press: New York, NY, USA, 2008.
136. Kubiak, K.; Fouvry, S.; Marechal, A.M.; Vernet, J.M. Behaviour of shot peening combined with WC–Co HVOF coating under complex fretting wear and fretting fatigue loading conditions. *Surf. Coat. Technol.* **2006**, *201*, 4323–4328. [CrossRef]

137. Junior, G.S.; Voorwald, H.J.C.; Vieira, L.F.S.; Cioffi, M.O.H.; Bonora, R.G. Evaluation of WC–10Ni thermal spray coating with shot peening on the fatigue strength of AISI 4340 steel. *Procedia Eng.* **2010**, *2*, 649–656. [CrossRef]
138. Hiegemann, L.; Weddeling, C.; BenKhalifa, N.; Tekkaya, A.E. Prediction of roughness after ball burnishing of thermally coated surfaces. *J. Mater. Process. Technol.* **2015**, *217*, 193–201. [CrossRef]
139. Mellor, B.G. *Surface Coatings for Protection Against Wear*; CRC Press: Boca Raton, FL, USA, 2006.
140. Pokhmurska, A.; Ciach, R. Microstructure and properties of laser treated arc sprayed and plasma sprayed coatings. *Surf. Coat. Technol.* **2000**, *125*, 415–418. [CrossRef]
141. Zhanga, S.H.; Yoon, J.H.; Li, M.X.; Cho, T.Y.; Joo, Y.K.; Cho, J.Y. Influence of CO_2 laser heat treatment on surface properties, electrochemical and tribological performance of HVOF sprayed WC–24%Cr_3C_2–6%Ni coating. *Mater. Chem. Phys.* **2010**, *119*, 458–464. [CrossRef]
142. Brandl, W.; Marginean, G.; Maghet, D.; Utu, D. Effects of specimen treatment and surface preparation on the isothermal oxidation behaviour of the HVOF-sprayed MCrAlY coatings. *Surf. Coat. Technol.* **2004**, *188–189*, 20–26. [CrossRef]
143. Shengzhi, H.; Dongyun, H.; Limin, Z. Microstructure and corrosion resistance of FeCrAl coating after high current pulsed electron beam surface modification. *Procedia Eng.* **2012**, *27*, 1700–1706.
144. Iwaszko, J.; Nitkiewicz, Z. Solidification microstructure of plasma sprayed and remelted carbide coatings (Cr_3C_2/Ni–Al, W2C–WC/Co). *Mater. Manuf. Process.* **2002**, *17*, 169–176. [CrossRef]
145. Gontarz, G.; Golański, D.; Chmielewski, T. Properties of Fe-Al Type intermetallic layers produced by AC TIG method. *Adv. Mater. Sci.* **2013**, *13*, 5–16. [CrossRef]
146. Garcia-Alonso, D.; Serres, N.; Demian, C.; Costil, S.; Langlade, C.; Coddet, C. Pre-/during-/post-laser processes to enhance the adhesion and mechanical properties of thermal-sprayed coatings with a reduced environmental impact. *J. Therm. Spray Technol.* **2011**, *20*, 719–735. [CrossRef]
147. Knuuttila, J.; Sorsa, P.; Mantyla, T. Sealing of thermal spray coatings by impregnation. *J. Therm. Spray Technol.* **1999**, *8*, 249–257. [CrossRef]
148. Kim, H.J.; Lee, C.H.; Kweon, Y.G. The effects of sealing on the mechanical properties of the plasma-sprayed alumina-titania coating. *Surf. Coat. Technol.* **2001**, *139*, 75–80. [CrossRef]
149. Ctibor, P.; Neufuss, K.; Zahalka, F.; Kolman, B. Plasma sprayed ceramic coatings without and with epoxy resin sealing treatment and their wear resistance. *Wear* **2007**, *262*, 1274–1280. [CrossRef]
150. Troczynski, T.; Yang, Q.; John, G. Post-deposition treatment of zirconia thermal barrier coatings using Sol-Gel alumina. *J. Therm. Spray Technol.* **1999**, *8*, 229–234. [CrossRef]
151. Caron, N.; Bianchi, L.; Methout, S. Development of a functional sealing layer for SOFC applications. *J. Therm. Spray Technol.* **2008**, *17*, 598–602. [CrossRef]
152. Casadei, F.; Tului, M. Combining thermal spraying and PVD technologies: A new approach of duplex surface engineering for Ti alloys. *Surf. Coat. Technol.* **2013**, *237*, 415–420. [CrossRef]
153. Kamiński, M.; Budzyński, P.; Szala, M.; Turek, M. Tribological properties of the Stellite 6 cobalt alloy implanted with manganese ions. *Mater. Sci. Eng.* **2018**, *421*, 032012. [CrossRef]
154. Steffens, H.D.; Wielage, B.; Drozak, J. Thermal spraying of composites—Manufacturing and post treatment. *Mikrochim. Acta* **1990**, *2*, 81–89. [CrossRef]
155. Verdian, M.M. Finishing and post-treatment of thermal spray coatings. In *Reference Module in Materials Science and Materials Engineering*; Hashimi, S., Ed.; Elsevier: Amsterdam, The Netherlands, 2016.
156. Kuribayashi, H.; Suganuma, K.; Miyamoto, Y.; Koizumi, M. Effects of HIP treatment on plasma sprayed ceramic coating onto stainless steel. *Ceram. Bull.* **1986**, *51*, 1031–1035.
157. Stoica, V.; Ahmed, R.; Golshan, M.; Tobe, S. Sliding wear evaluation of hot isostatically pressed thermal spray cermet coatings. *J. Therm. Spray Technol.* **2004**, *13*, 93–107. [CrossRef]
158. Burman, C.; Ericsson, T.; Kvernes, I.; Lindblom, Y. Coatings with lenticular oxides preventing interdiffusion. *Surf. Coat. Technol.* **1987**, *32*, 127–140. [CrossRef]
159. Khor, K.A.; Loh, N.L. Hot isostatic pressing of plasma sprayed Ni-base alloys. *J. Therm. Spray Technol.* **1994**, *3*, 57–62. [CrossRef]
160. Prawara, B.; Yara, H.; Miyagi, Y.; Fukushima, T. Spark plasma sintering as a post-spray treatment for thermally sprayed coatings. *Surf. Coat. Technol.* **2003**, *162*, 234–241. [CrossRef]
161. Murakami, T.; Sasaki, S.; Ito, K.; Inu, H.; Yamaguchi, M. Microstructure of Nb substrates coated with Mo_4Si_1 Al_{52}–Al_2O_3 composite and B-doped Mo_5Si_3 layers by spark plasma sintering. *Intermetallics* **2004**, *12*, 749–754. [CrossRef]

162. Chraska, T.; Pala, Z.; Musalek, R.; Medricky, J.; Vilemova, M. Post-treatment of plasma-sprayed amorphous ceramic coatings by spark plasma sintering. *J. Therm. Spray Technol.* **2015**, *24*, 637–643. [CrossRef]
163. Vuoristo, P. 4.10—Thermal spray coating processes. In *Comprehensive Materials Processing*; Hashmi, S., Batalha, G.F., Van Tyne, C.J., Yilbas, B., Eds.; Elsevier: Oxford, UK, 2014; pp. 229–276.
164. Nouri, A.; Sola, A. Powder morphology in thermal spraying. *J. Adv. Manuf. Process.* **2019**, *1*, e10020.
165. Herman, H. Powders for thermal spray technology. *KONA Powder Part. J.* **1991**, *9*, 187–199. [CrossRef]
166. Dietrich, S.; Wunderer, M.; Huissel, A.; Zaeh, M.F. A new approach for a flexible powder production for additive manufacturing. *Procedia Manuf.* **2016**, *6*, 88–95. [CrossRef]
167. Wisutmethangoon, S.; Plookphol, T.; Sungkhaphaitoon, P. Production of SAC305 powder by ultrasonic atomization. *Powder Technol.* **2011**, *209*, 105–111. [CrossRef]
168. Kobayashi, A.; Yano, S.; Kimura, H.; Inoue, A. Fe-based metallic glass coatings produced by smart plasma spraying process. *Mater. Sci. Eng. B* **2008**, *148*, 110–113. [CrossRef]
169. Santana, D.D.A.; Kiminami, C.S.; Coury, F.G.; Liberato, G.L.; Gargarella, P.; Kaufman, M.J. Consolidation of Fe-based metallic glass powders by hot pressing. *Mater. Res.* **2019**, *22*, e20180581. [CrossRef]
170. Lee, P.-Y.; Lin, C.-K.; Jeng, I.-K.; Wang, C.-C.; Chen, G.-S. Characterization of Ni57Zr20Ti18Al5 amorphous powder obtained by mechanical alloying. *Mater. Chem. Phys.* **2004**, *84*, 358–362. [CrossRef]
171. Fujii, N.; Nishizawa, R.; Nabeta, T. Spinel Powder and Manufacturing Process Therefor, and Processes for Producing Thermal Spraying Film and Gas Sensor Elements. U.S. Patent 9340680B2, 17 May 2016.
172. Fauchais, P.; Montavon, G.; Lima, R.S.; Marple, B.R. Engineering a new class of thermal spray nano-based microstructures from agglomerated nanostructured particles, suspensions and solutions: An invited review. *J. Phys. Appl. Phys.* **2011**, *44*, 93001. [CrossRef]
173. Moreno, R.; Bannier, E. Feedstock suspensions and solutions. In *Future Development of Thermal Spray Coatings*; Espallargas, N., Ed.; Woodhead Publishing: Cambridge, UK, 2015; pp. 51–80.
174. Sokołowski, P.; Kozerski, S.; Pawłowski, L.; Ambroziak, A. The key process parameters influencing formation of columnar microstructure in suspension plasma sprayed zirconia coatings. *Surf. Coat. Technol.* **2014**, *260*, 97–106. [CrossRef]
175. Berger, L.-M.; Toma, F.-L.; Potthoff, A. Thermal spraying with suspensions-an economic spray process. *Therm. Spray Bull.* **2013**, *65*, 98–101.
176. Toma, F.-L.; Potthoff, A.; Berger, L.-M.; Leyens, C. Demands, potentials, and economic aspects of thermal spraying with suspensions: A critical review. *J. Therm. Spray Technol.* **2015**, *24*, 1143–1152. [CrossRef]
177. Vardelle, A.; Moteau, C.; Vuoristo, P. The 2016 thermal spray roadmap. *J. Therm. Spray Technol.* **2016**, *25*, 1376–1440. [CrossRef]
178. Potthoff, A.; Kratzsch, R.; Barbosa, M.; Kulissa, N.; Kunze, O.; Toma, F.-L. Development and application of binary suspensions in the ternary system Cr_2O_3-TiO_2-Al_2O_3 for S.-HVOF spraying. *J. Therm. Spray Technol.* **2018**, *27*, 710–717. [CrossRef]
179. Molina, T.; Vicent, M.; Sánchez, E.; Moreno, R. Dispersion and reaction sintering of alumina–titania mixtures. *Mater. Res. Bull.* **2012**, *47*, 2469–2474. [CrossRef]
180. Carpio, P.; Candidato, R.T.; Pawłowski, L.; Salvador, M.D. Solution concentration effect on mechanical injection and deposition of YSZ coatings using the solution precursor plasma spraying. *Surf. Coat. Technol.* **2019**, *371*, 124–130. [CrossRef]
181. Jordan, E.; Gell, M. Compositionally Graded and Porosity Graded Coatings Using a Solution Precursor Plasma Spray Process. U.S. Patent 20190301000A1, 3 October 2019.
182. Meng, X.; Li, E.; Huang, W.; Bai, Y.; Ma, W.; Wang, R. Thermal decomposition and crystallization behavior of double rare-earth co-doped $SrZrO_3$ precursor used in the solution precursor plasma spray process. *Surf. Coat. Technol.* **2019**, *369*, 87–94. [CrossRef]
183. Sergi, R.; Bellucci, D.; Candidato, R.T.; Lusvarghi, L.; Bollelli, G.; Pawłowski, L.; Candiani, G.; Altomare, L.; De Nardo, L.; Cannillo, V. Bioactive Zn-doped hydroxyapatite coatings and their antibacterial efficacy against *Escherichia coli* and *Staphylococcus aureus*. *Surf. Coat. Technol.* **2018**, *352*, 84–91. [CrossRef]
184. Unabia, R.B.; Bonebeau, S.; Candidato, R.T.; Jouin, J.; Noguera, O.; Pawłowski, L. Investigation on the structural and microstructural properties of copper-doped hydroxyapatite coatings deposited using solution precursor plasma spraying. *J. Eur. Ceram. Soc.* **2019**, *39*, 4255–4263. [CrossRef]
185. Joshi, S.V.; Sivakumar, G.; Raghuveer, T.; Dusane, R.O. Hybrid plasma-sprayed thermal barrier coatings using powder and solution precursor feedstock. *J. Therm. Spray Technol.* **2014**, *23*, 616–624. [CrossRef]
186. Thorpe, M.L. Thermal spray: Industry in transition. *Adv. Mater. Process.* **1993**, *143*, 50–61.

187. Hasan, F.; Wang, J.; Berndt, C. Determination of the mechanical properties of plasma-sprayed hydroxyapatite coatings using the knoop indentation technique. *J. Therm. Spray Technol.* **2015**, *24*, 865–877. [CrossRef]
188. Asthana, R.; Kumar, A.; Dahotre, N.B. *Materials Science in Manufacturing*; Elsevier Science and Technology Books: Amsterdam, The Netherlands, 2006.
189. Leigh, S.H.; Berndt, C.C. A test for coating adhesion on flat substrates—A technical note. *J. Therm. Spray Technol.* **1994**, *3*, 184–190. [CrossRef]
190. Marot, G.; Lesage, J.; Demarecaux, P.; Hadad, M.; Siegman, S.; Staia, M.H. Interfacial indentation and shear tests to determine the adhesion of thermal spray coatings. *Surf. Coat. Technol.* **2006**, *201*, 2080–2085. [CrossRef]
191. Shankar, N.R.; Berndt, C.C.; Herman, H. Characterization of the mechanical properties of plasma-sprayed coatings. *Mater. Sci. Res.* **1983**, *15*, 473–489.
192. Białucki, P.; Kozerski, S. Study of adhesion of different plasma-sprayed coatings to aluminium. *Surf. Coat. Technol.* **2006**, *201*, 2061–2064. [CrossRef]
193. Grutzner, H.; Weiss, H. A novel shear test for plasma-sprayed coatings. *Surf. Coat. Technol.* **1991**, *45*, 317–323. [CrossRef]
194. Era, H.; Otsubo, F.; Uchida, T.; Fukuda, S.; Kishitake, K. A modified shear test for adhesion evaluation of thermal sprayed coating. *Mater. Sci. Eng. A* **1998**, *251*, 166–172. [CrossRef]
195. Berndt, C.C.; McPherson, R. A fracture mechanics approach to the adhesion of flame and plasma sprayed coatings. *Trans. Int. Eng.* **1981**, *6*, 53–58.
196. Berndt, C.C.; Lin, C.K. Measurement of adhesion for thermally sprayed materials. *J. Adhes. Sci. Technol.* **1993**, *7*, 1235–1264. [CrossRef]
197. Clyne, T.W.; Gill, S.C. Residual stresses in thermal spray coatings and their effect on interfacial adhesion: A review of recent work. *J. Therm. Spray. Technol.* **1996**, *5*, 401–418. [CrossRef]
198. Du, H.; Hua, W.; Liu, J.; Gong, J.; Sun, C.; Wen, L. Influence of process variables on the qualities of detonation gun sprayed WC–Co coatings. *Mater. Sci. Eng. A* **2005**, *408*, 202–210. [CrossRef]
199. Bernardie, R.; Berkouch, R.; Valette, S.; Absi, J.; Lefort, P. Experimental and numerical study of a modified ASTM C633 adhesion test for strongly bonded coatings. *J. Mech. Sci. Technol.* **2017**, *31*, 3241–3247. [CrossRef]
200. Schmidt, T.; Gartner, F.; Assadi, H.; Kreye, H. Development of a generalized parameter window for cold spray deposition. *Acta Mater.* **2006**, *54*, 729–742. [CrossRef]
201. Sexsmith, M.; Troczyński, T. Peel adhesion test for thermal spray coating. *J. Therm. Spray Technol.* **1994**, *3*, 404–411. [CrossRef]
202. Kishi, A.; Kuroda, S.; Inoue, T.; Fukushima, T.; Yumoto, H. Tensile test specimens with a circumferential precrack for evaluation of interfacial toughness of thermal-sprayed coatings. *J. Therm. Spray Technol.* **2008**, *17*, 228–233. [CrossRef]
203. Bolis, C.; Berthe, L.; Boustie, M.; Arrigoni, M.; Barradas, S.; Jeandin, M. Physical approach of adhesion test using laser driven shock wave. *J. Phys. D Appl. Phys.* **2007**, *40*, 3155–3163. [CrossRef]
204. Chicot, D.; Demarecaux, P.; Lesage, J. Apparent interface toughness of substrate and coatings couples from indentation tests. *Thin Solid Films* **1996**, *283*, 151–157. [CrossRef]
205. Kozerski, S.; Łatka, L.; Pawłowski, L.; Cernuschi, F.; Petit, F.; Pierlot, C.; Podlesak, H.; Laval, J.P. Preliminary study on suspension plasma sprayed ZrO_2 + 8 wt.% Y_2O_3 coatings. *J. Eur. Ceram. Soc.* **2011**, *31*, 2089–2098. [CrossRef]
206. Ang, A.; Berndt, C.C. A review of testing methods for thermal spray coatings. *Int. Mater. Rev.* **2014**, *59*, 179–223. [CrossRef]
207. Hermann, K. *Hardness Testing, Principles and Applications*; ASM International: Materials Park, OH, Canada, 2011.
208. Walley, S.M. Historical origins of indentation hardness testing. *Mater. Sci. Technol.* **2012**, *28*, 1028–1044. [CrossRef]
209. Pelleg, J. *Mechanical Properties of Materials*; Springer Science and Business Media: Dordrecht, The Netherlands, 2013.
210. Alcala, J.; Gaudette, F.; Suresh, S.; Sampath, S. Instrumented spherical micro-indentation of plasma-sprayed coatings. *Mater. Sci. Eng. A* **2001**, *316*, 1–10. [CrossRef]
211. Dey, A.; Mukhopadhyay, A.K.; Gangadharan, S.; Sinha, M.K.; Basu, D. Weibull modulus of nano-hardness and elastic modulus of hydroxyapatite coating. *J. Mater. Sci.* **2009**, *44*, 4911–4918. [CrossRef]
212. Lin, C.K.; Berndt, C.C. Statistical analysis of microhardness variations in thermal spray coatings. *J. Mater. Sci.* **1995**, *30*, 111–117. [CrossRef]
213. Valente, T. Statistical evaluation of Vicker's indentation test results for thermally sprayed materials. *Surf. Coat. Technol.* **1997**, *90*, 14–20. [CrossRef]
214. Oliver, W.C.; Pharr, G.M. An improved technique for determining hardness and elastic modulus using load and displacement sensing indentation experiments. *J. Mater. Res.* **1992**, *7*, 1564–1583. [CrossRef]

215. Łatka, L.; Chicot, D.; Cattini, A.; Pawłowski, L.; Ambroziak, A. Modeling of elastic modulus and hardness determination by indentation of porous yttria stabilized zirconia coatings. *Surf. Coat. Technol.* **2013**, *220*, 131–139. [CrossRef]
216. McPherson, R. A review of microstructure and properties of plasma sprayed ceramic coatings. *Surf. Coat. Technol.* **1989**, *39*, 173–181. [CrossRef]
217. Marshall, D.B.; Noma, T.; Evans, A.G. A simple method for determining elastic-modulus-to-hardness ratios using Knoop indentation measurements. *J. Am. Ceram. Soc.* **1982**, *65*, c175–c176. [CrossRef]
218. Łatka, L.; Cattini, A.; Chicot, D.; Pawłowski, L.; Kozerski, S.; Petit, F.; Denoirjean, A. Mechanical properties of yttria-and ceria-stabilized zirconia coatings obtained by suspension plasma spraying. *J. Therm. Spray Technol.* **2013**, *22*, 125–130. [CrossRef]
219. Choi, S.R.; Zhu, D.; Miller, R.A. Mechanical properties/database of plasma-sprayed ZrO_2-8wt% Y_2O_3 thermal barrier coatings. *Int. J. Appl. Ceram. Technol.* **2004**, *1*, 330–342. [CrossRef]
220. Kovarik, O.; Siegl, J.; Nohava, J.; Chraska, P. Young's modulus and fatigue behavior of plasma-sprayed alumina coatings. *J. Therm. Spray Technol.* **2005**, *14*, 231–238. [CrossRef]
221. Wang, W.Z.; Li, C.J.; Wang, Y.Y. Effect of spray distance on the mechanical properties of plasma sprayed Ni-45Cr coatings. *Mater. Trans.* **2006**, *47*, 1643–1648. [CrossRef]
222. Bolelli, G.; Candeli, A.; Koivuluoto, H.; Lusvarghi, L.; Manfredini, T.; Vuoristo, P. Microstructure-based thermo-mechanical modelling of thermal spray coatings. *Mater. Des.* **2015**, *73*, 20–34. [CrossRef]
223. Thompson, J.A.; Clyne, T.W. The effect of heat treatment on the stiffness of zirconia topcoats in plasma sprayed TBCs. *Acta Mater.* **2001**, *49*, 1565–1575. [CrossRef]
224. Matejicek, J.; Sampath, S. In situ measurement of residual stresses and elastic moduli in thermal sprayed coatings: Part 1: Apparatus and analysis. *Acta Mater.* **2003**, *51*, 863–872. [CrossRef]
225. Tan, Y.; Shyam, A.; Choi, W.B.; Lara-Curzio, E.; Sampath, S. Anisotropic elastic properties of thermal spray coatings determined via resonant ultrasound spectroscopy. *Acta Mater.* **2010**, *58*, 5305–5315. [CrossRef]
226. Lima, R.S.; Kruger, S.E.; Marple, B.R. Towards engineering isotropic behavior of mechanical properties in thermally sprayed ceramic coatings. *Surf. Coat. Technol.* **2008**, *202*, 3643–3652. [CrossRef]
227. Liu, A.F. *Mechanics and Mechanisms of Fracture: An Introduction*; ASM International: Materials Park, OH, USA, 2005.
228. Guo, D.Z.; Wang, L.J. Measurements of the critical strain energy release rate of plasma-sprayed coatings. *Surf. Coat. Technol.* **1992**, *56*, 19–25. [CrossRef]
229. Chattopadhyay, R. *Surface Wear: Analysis, Treatment, and Preventions*; ASM International: Materials Park, OH, USA, 2001.
230. Wood, R.J.K.; Roy, M. Tribology of thermal sprayed coatings. In *Surface Engineering for Enhanced Performance Against Wear*; Roy, M., Ed.; Springer: Berlin/Heidelberg, Germany, 2012.
231. Dwivedi, D.K. *Surface Engineering—Enhancing Life of Tribological Components*; Springer: Berlin/Heidelberg, Germany, 2018.
232. Yanga, Q.; Senda, T.; Hirose, A. Sliding wear behavior of WC–12% Co coatings at elevated temperatures. *Surf. Coat. Technol.* **2006**, *200*, 4208–4212. [CrossRef]
233. Myalska, H.; Lusvarghi, L.; Bolelli, G.; Sassatelli, P.; Moskal, G. Tribological behavior of WC-Co HVAF-sprayed composite coatings modified by nano-sized TiC addition. *Surf. Coat. Technol.* **2019**, *371*, 401–416. [CrossRef]
234. Gawne, D.T.; Qiu, Z.; Bao, Y.; Zhang, T.; Zhang, K. Abrasive wear resistance of plasma sprayed glass-composite coatings. *J. Therm. Spray Technol.* **2001**, *10*, 599–603. [CrossRef]
235. Magnani, M.; Suegama, P.H.; Espallargas, N.; Fugivara, C.S.; Dosta, S.; Guilemany, J.M.; Benedettir, A.V. Corrosion and wear studies of Cr3C2-NiCr-HVOF coatings sprayed on AA7050T7 under cooling. *J. Therm. Spray Technol.* **2009**, *18*, 354–363. [CrossRef]
236. Mann, B.S.; Arya, V. Abrasive and erosive wear characteristics of plasma nitriding and HVOF coatings: Their application in hydro turbines. *Wear* **2001**, *249*, 354–360. [CrossRef]
237. Ji, G.C.; Li, C.J.; Wang, Y.Y.; Li, W.Y. Erosion performance of HVOF-sprayed Cr_3C_2-NiCr coatings. *J. Therm. Spray Technol.* **2007**, *16*, 557–565. [CrossRef]
238. Ahmed, R.; Hadfield, M. Mechanisms of fatigue failure in thermal spray coatings. *J. Therm. Spray Technol.* **2002**, *11*, 334–349. [CrossRef]
239. Koiprasert, H.; Dumrongrattana, S.; Niranatlumpong, P. Thermally sprayed coatings for protection of fretting wear in land-based gas-turbine engine. *Wear* **2004**, *257*, 1–7. [CrossRef]
240. Basak, A.K.; Matteazzi, P.; Vardavoulias, M.; Celis, J.P. Corrosion–wear behavior of thermal sprayed nanostructured FeCu/WC–Co coatings. *Wear* **2006**, *261*, 1042–1050. [CrossRef]
241. Mellor, B.G. *Surface Coatings for Protection Against Wear*; Woodhead Publishing Limited: Cambridge, UK, 2006.

242. Holmberg, K.; Matthews, A. *Coatings Tribology—Properties, Mechanisms, Techniques and Applications in Surface Engineering*; Elsevier: Amsterdam, The Netherlands, 2009.
243. Greving, D.J.; Shadley, R.J.; Rybicki, E.F. Effects of coating thickness and residual stresses on the bond strength of ASTM C633-79 thermal spray coating test specimens. *J. Therm. Spray Technol.* **1994**, *3*, 371. [CrossRef]
244. Gupta, A.; Talha, M. Recent development in modeling and analysis of functionally graded materials and structures. *Prog. Aerosp. Sci.* **2015**, *79*, 1–14. [CrossRef]
245. Rowe, R.H., Jr.; Lare, P.J.; Hahn, H. Surgical Implant Having a Graded Porous Coating. U.S. Patent 4542539A, 24 September 1985.
246. Mahamood, R.M.; Akinlabi, E.T. *Functionally Graded Materials*; Springer: Berlin/Heidelberg, Germany, 2017.
247. Khor, K.A.; Gu, Y.W. Effects of residual stress on the performance of plasma sprayed functionally graded ZrO_2/NiCoCrAlY coatings. *Mater. Sci. Eng. A* **2000**, *277*, 64–76. [CrossRef]
248. Ge, W.A.; Zhao, C.Y.; Wang, B.X. Thermal radiation and conduction in functionally graded thermal barrier coatings. Part II: Experimental thermal conductivities and heat transfer modeling. *Int. J. Heat Mass Transf.* **2019**, *134*, 166–174. [CrossRef]
249. Khor, K.A.; Gu, Y.W. Thermal properties of plasma-sprayed functionally graded thermal barrier coatings. *Thin Solid Films* **2000**, *372*, 104–113. [CrossRef]
250. Baig, M.N.; Khalid, F.A.; Khan, F.N.; Rehman, K. Properties and residual stress distribution of plasma sprayed magnesia stabilized zirconia thermal barrier coatings. *Ceram. Int.* **2014**, *40*, 4853–4868. [CrossRef]
251. Carpio-Cobo, P.; Salvador Moya, M.D.; Borrell, T.M.A.; Sánchez, E. Thermal behaviour of multilayer and functionally graded YSZ/$Gd_2Zr_2O_7$ coatings. *Ceram. Int.* **2017**, *43*, 4048–4054. [CrossRef]
252. Znamirowski, Z.; Kozerski, S.; Łatka, L.; Pawłowski, L. The influence of the surface preparation on field electron emission of the TiO_2 coatings manufactured by suspension plasma spraying. *Weld. Technol. Rev.* **2016**, *88*, 27–31.
253. Xu, N.S.; Ejaz Huq, S. Novel cold cathode materials and applications. *Mater. Sci. Eng. R* **2005**, *48*, 47–189. [CrossRef]
254. Tomaszek, R.; Znamirowski, Z.; Pawłowski, L.; Wojnakowski, A. Temperature behavior of Titania field emitters realized by suspension plasma spraying. *Surf. Coat. Technol.* **2006**, *201*, 2099–2102. [CrossRef]
255. Znamirowski, Z.; Czarczyński, W.; Pawłowski, L.; Wojnakowski, A. Temperature influence and hot electrons in field electron emission from composite layers deposited by air plasma spraying of powders and suspensions. *J. Vac. Sci. Technol. B* **2007**, *25*, 1664–1670. [CrossRef]
256. Czarczyński, W.; Znamirowski, Z. Field electron emission experiments with plasma sprayed layers. *Surf. Coat. Technol.* **2008**, *202*, 4422–4427. [CrossRef]
257. Pawlowski, L. The relationship between structure and dielectric properties in plasma sprayed alumina coatings. *Surf. Coat. Technol.* **1988**, *35*, 285–298. [CrossRef]
258. Turunen, E.; Varis, T.; Hannula, S.-P.; Vaidya, A.; Kulkarni, A.; Gutleber, J.; Sampath, S.; Herman, H. On the role of particle state and deposition procedure on mechanical, tribological and dielectric response of high velocity oxy-fuel sprayed alumina coatings. *Mat. Sci. Eng. A* **2006**, *415*, 1–11. [CrossRef]
259. Swindeman, C.J.; Seals, R.D.; Murray, W.P.; Cooper, M.H.; Whit, R.L. An investigation of the electrical behavior of thermally sprayed aluminum oxide. In Proceedings of the 9th National Thermal Spray Conference, Cincinnati, OH, USA, 7–11 October 1996; pp. 793–797.
260. Niittymäki, M.; Lahti, K.; Suhonen, T.; Metsäjoki, J. Effect of temperature and humidity on dielectric properties of thermally sprayed alumina coatings. *IEEE Trans. Dielectr. Electr. Insul.* **2018**, *25*, 908–918. [CrossRef]
261. Toma, F.L.; Berger, L.M.; Scheitz, S.; Langner, S.; Potthoff, C.R.A.; Sauchuk, V.; Kusnezoff, M. Comparison of the microstructural characteristics and electrical properties of thermally sprayed Al_2O_3 coatings from aqueous suspensions and feedstock powders. *J. Therm. Spray Technol.* **2012**, *21*, 480–488. [CrossRef]
262. Łatka, L.; Pawłowski, L.; Kozerski, S.; Toma, F.L.; Leupolt, B.; Berger, L.M. Photocatalytic properties of suspension plasma sprayed TiO_2 coatings obtained on different substrates. W: Surface modification technologies XXIV. In Proceedings of the Twenty Fourth International Conference on Surface Modification Technologies, Dresden, Germany, 7–9 September 2010; pp. 95–106.
263. Kozerski, S.; Toma, F.L.; Pawłowski, L.; Leupolt, B.; Łatka, L.; Berger, L.M. Suspension plasma sprayed TiO_2 coatings using different injectors and their photocatalytic properties. *Surf. Coat. Technol.* **2010**, *205*, 980–986. [CrossRef]
264. Toma, F.L.; Berger, L.M.; Stahr, C.C.; Naumann, T.; Langner, S. Microstructures and functional properties of suspension sprayed Al_2O_3 and TiO_2 coatings: An overview. *J. Therm. Spray Technol.* **2010**, *19*, 262–274. [CrossRef]
265. Yang, G.J.; Li, C.J.; Han, F.; Ohmori, A. Microstructure and photocatalytic performance of high velocity oxy-fuel sprayed T_iO_2 coatings. *Thin Solid Film.* **2004**, *466*, 81–85. [CrossRef]

266. Ohmori, A.; Shoyama, H.; Matsusaka, S.; Ohashi, K.; Moriya, K.; Li, C.J. Study of photo-catalytic character of plasma sprayed TiO_2 coatings, thermal spray: Surface engineer. Via Applied Research. In *Proceedings of the 1st International Thermal Spray Conference*; Berndt, C.C., Ed.; ASM International: Geauga, OH, Canada, 2000; pp. 317–323.
267. Murphy, W.; Black, J.; Hastings, G. *Handbook of Biomaterial Properties*, 2nd ed.; Springer: Berlin/Heidelberg, Germany, 2016.
268. Ratner, B.D.; Hoffmann, A.S.; Schoen, F.J.; Lemons, E.J. *Biomaterials Science—An Introduction to Materials in Medicine*, 2nd ed.; Elsevier: Amsterdam, The Netherlands, 2004.
269. Hench, L.L. *An Introduction to Bioceramics*, 2nd ed.; Imperial College Press: London, UK, 2013.
270. Heimann, R.B. Plasma-sprayed hydroxyapatite-based coatings: Chemical, mechanical, microstructural and biomedical properties. *J. Therm. Spray Technol.* **2016**, *25*, 827–850. [CrossRef]
271. Heimann, R.B. Structure, properties, and biomedical performance of osteoconductive bioceramic coatings. *Surf. Coat. Technol.* **2013**, *233*, 27–38. [CrossRef]
272. Ibrahim, M.Z.; Sarhan, A.A.D.; Yusuf, F.; Hamdi, M. Biomedical materials and techniques to improve the tribological, mechanical and biomedical properties of orthopedic implants—A review article. *J. Alloys Compd.* **2017**, *714*, 636–667. [CrossRef]
273. Henao, J.; Poblano-Salas, C.; Monsalve, M.; Corona-Casteura, J.; Barceinas-Sanchez, O. Bio-active glass coatings manufactured by thermal spray: A status report. *J. Mater. Res. Technol.* **2019**, *8*, 4965–4984. [CrossRef]
274. Habibovic, P.; Barrere, F.; Blitterswijk, C.A.; Groot, K.; Layrolle, P. Biomimetic hydroxyapatite coating on metal implants. *J. Am. Ceram. Soc.* **2002**, *85*, 517–522. [CrossRef]
275. Yilmaz, B.; Evis, Z. Biomimetic coatings of calcium phosphates on titanium alloys. In *Biomedical Nanomaterials, From Design to Implementation*; The Institution of Engineering and Technology: Stevenage, UK, 2016.
276. Kokubo, T.; Kushitani, H.; Sakka, S.; Kitsugi, T.; Yamamuro, T. Solutions able to reproduce in vivo surface-structure change in bioactive glass-ceramic A-W^3. *J. Biomed. Mater. Res.* **1990**, *24*, 721–734. [CrossRef]
277. Duan, K.; Tang, A.; Wang, R. A new evaporation-based method for the preparation of biomimetic calcium phosphate coatings on metals. *Mater. Sci. Eng. C* **2009**, *29*, 334–1337. [CrossRef]
278. Choi, J.; Bogdanski, D.; Koller, M.; Esenwein, S.A.; Muller, D.; Muhr, G.; Epple, M. Calcium phosphate coating of nickel–titanium shape-memory alloys. Coating procedure and adherence of leukocytes and platelets. *Biomaterials* **2003**, *24*, 3689–3696. [CrossRef]
279. Chen, C.; Kong, X.; Zhang, S.M.; Lee, I.S. Characterization and in vitro biological evaluation of mineral/osteogenic growth peptide nanocomposites synthesized biomimetically on titanium. *Appl. Surf. Sci.* **2015**, *334*, 62–68. [CrossRef]
280. Cattini, A.; Łatka, L.; Bellucci, D.; Bolelli, G.; Sola, A.; Lusvarghi, L.; Pawłowski, L.; Cannillo, V. Suspension plasma sprayed bioactive glass coatings: Effects of processing on microstructure, mechanical properties and in-vitro behaviour. *Surf. Coat. Technol.* **2013**, *220*, 52–59. [CrossRef]
281. Łatka, L.; Pawłowski, L.; Chicot, D.; Pierlot, C.; Petit, F. Mechanical properties of suspension plasma sprayed hydroxyapatite coatings submitted to simulated body fluid. *Surf. Coat. Technol.* **2010**, *205*, 954–960. [CrossRef]
282. Xu, H.; Geng, X.; Liu, G.; Xiao, J.; Li, D.; Zhang, Y.; Zhu, P.; Zhang, C. Deposition, nanostructure and phase composition of suspension plasma-sprayed hydroxyapatite coatings. *Ceram. Int.* **2016**, *42*, 8684–8690. [CrossRef]
283. Khun, N.W.; Li, Z.; Khor, K.A.; Cizek, J. Higher in-flight particle velocities enhance in vitro tribological behaviour of plasma sprayed hydroxyapatite coatings. *Tribol. Int.* **2016**, *103*, 496–503. [CrossRef]
284. Pizzoferrato, A.; Ciapetti, G.; Stea, S.; Cenni, E.; Arciola, C.R.; Granchi, D.; Savarino, L. Cell culture methods for testing biocompatibility. *Clin. Mater.* **1994**, *15*, 173–190. [CrossRef]
285. Lee, J.T.Y.; Leng, Y.; Chow, K.L.; Ren, F.; Ge, X.; Wang, K.; Lu, X. Cell culture medium as an alternative to conventional simulated body fluid. *Acta Biomater.* **2011**, *7*, 2615–2622. [CrossRef]
286. Amaral, M.; Gomes, P.S.; Lopes, M.A.; Santos, J.D.; Silva, R.F.; Fernandes, M.H. Cytotoxicity evaluation of nanocrystalline diamond coatings by fibroblast cell cultures. *Acta Biomater.* **2009**, *5*, 755–763. [CrossRef]
287. Clarke, D.R.; Oechsner, M.; Padture, N.P. Thermal-barrier coatings for more efficient gas-turbine engines. *MRS Bull.* **2012**, *37*, 891–898. [CrossRef]
288. Łatka, L. Thermal barrier coatings manufactured by suspension plasma spraying—A review. *Adv. Mater. Sci.* **2018**, *18*, 95–117. [CrossRef]
289. Evans, H.E. Oxidation failure of TBC systems: An assessment of mechanisms. *Surf. Coat. Technol.* **2011**, *206*, 1512–1521. [CrossRef]

290. Ali, I.; Sokołowski, P.; Grund, T.; Pawłowski, L.; Lampke, T. Oxidation behavior of thermal barrier coating systems with Al interlayer under isothermal loading. In Proceeding of the 20th Chemnitz Seminar on Materials Engineering—20 Werkstofftechnisches Kolloquium (previous editions: WTK-2016, WTK-2017), Chemnitz, Germany, 14–15 March 2018.
291. Sampath, S.; Herman, H.; Shimoda, N.; Saito, T. Thermal spray processing of FGMs. *MRS Bull.* **1995**, *20*, 27–31. [CrossRef]
292. Jian, C.Y.; Hashida, T.; Takahashi, H.; Saito, M. Thermal shock and fatigue resistance evaluation of functionally graded coating for gas turbine blades by laser heating method. *Compos. Eng.* **1995**, *5*, 879–889. [CrossRef]
293. Ge, W.A.; Zhao, C.Y.; Wang, B.X. Thermal radiation and conduction in functionally graded thermal barrier coatings. Part I: Experimental study on radiative properties. *Int. J. Heat Mass Transf.* **2019**, *134*, 101–113. [CrossRef]
294. Kokini, K.; DeJonge, J.; Rangaraj, S.; Beardsley, B. Thermal shock of functionally graded thermal barrier coatings with similar thermal resistance. *Surf. Coat. Technol.* **2002**, *154*, 223–231. [CrossRef]
295. Samani, T.; Kermani, M.; Razavi, M.; Farvizi, M.; Mobasherpour, I. A comparative study on the microstructure, hot corrosion behavior and mechanical properties of duplex and functionally graded nanostructured/conventional YSZ thermal barrier coatings. *Mater. Res. Express* **2019**, *6*, 115063. [CrossRef]
296. Carpio, P.; Rayón, E.; Salvador, M.D.; Lusvarghi, L.; Sánchez, E. Mechanical properties of double-layer and graded composite coatings of YSZ obtained by atmospheric plasma spraying. *J. Therm. Spray Technol.* **2016**, *25*, 778–787. [CrossRef]
297. Khoddami, A.M.; Sabour, A.; Hadavi, S.M.M. Microstructure formation in thermally sprayed duplex and functionally graded NiCrAlY/Yttria-Stabilized Zirconia coatings. *Surf. Coat. Technol.* **2007**, *201*, 6019–6024. [CrossRef]
298. Lashmi, P.G.; Ananthapadmanabhan, P.V.; Unnikrishnan, G.; Aruna, S.T. Present status and future prospects of plasma sprayed multilayered thermal barrier coating systems. *J. Eur. Ceram. Soc.* **2020**, *40*, 2731–2745. [CrossRef]
299. Viswanathan, V.; Dwivedi, G.; Sampath, S. Engineered multilayer thermal barrier coatings for enhanced durability and functional performance. *J. Am. Ceram. Soc.* **2014**, *97*, 2770–2778. [CrossRef]
300. Chen, H.; Liu, Y.; Gao, Y.; Tao, S.; Luo, H. Design, preparation, and characterization of graded YSZ/$La_2Zr_2O_7$ thermal barrier coatings. *J. Am. Ceram. Soc.* **2010**, *93*, 1732–1740.
301. Guo, H.; Wang, Y.; Wang, L.; Gong, S. Thermo-physical properties and thermal shock resistance of segmented $La_2Ce_2O_7$/YSZ thermal barrier coatings. *J. Therm. Spray Technol.* **2009**, *18*, 665–671. [CrossRef]
302. Chen, X.; Gu, L.; Zou, B.; Wang, Y.; Cao, X. New functionally graded thermal barrier coating system based on $LaMgAl_{11}O_{19}$/YSZ prepared by air plasma spraying. *Surf. Coat. Technol.* **2012**, *206*, 2265–2274. [CrossRef]
303. Kirbiyik, F.; Gok, M.G.; Goller, G. Microstructural, mechanical and thermal properties of Al_2O_3/CYSZ functionally graded thermal barrier coatings. *Surf. Coat. Technol.* **2017**, *329*, 193–201. [CrossRef]
304. Gok, M.G.; Goller, G. Production and characterisation of GZ/CYSZ alternative thermal barrier coatings with multilayered and functionally graded designs. *J. Eur. Ceram. Soc.* **2016**, *36*, 1755–1764.
305. Li, C.-J.; Li, Y.; Yang, G.-J.; Li, C.-X. A novel plasma-sprayed durable thermal barrier coating with a well-bonded YSZ interlayer between porous YSZ and bond coat. *J. Therm. Spray Technol.* **2012**, *21*, 383–390. [CrossRef]
306. Li, H. Thermal sprayed bioceramic coatings: Nanostructured hydroxyapatite (HA) and HA-based composites. In *Biological and Biomedical Coatings Handbook*; Zhang, S., Ed.; CRC Press: Boca Raton, FL, USA, 2011.
307. Ratner, B.D.; Hoffman, A.S.; Schoen, F.J.; Lemons, J.E. Biomaterials science: A multidisciplinary endeavor. In *Biomaterials Science*; Ratner, B.D., Hoffman, A.S., Schoen, F.J., Lemons, J.E., Eds.; Elsevier Academic Press: San Diego, CA, USA, 2013.
308. Wang, Y.; Khor, K.A.; Cheang, P. Thermal spraying of functionally graded calcium phosphate coatings for biomedical implants. *J. Therm. Spray Technol.* **1998**, *7*, 50–57. [CrossRef]
309. Khor, K.A.; Wang, Y.; Cheang, P. Thermal spraying of functionally graded coatings for biomedical applications. *Surf. Eng.* **1998**, *14*, 159–164. [CrossRef]
310. Wang, M.; Yang, X.Y.; Khor, K.A.; Wang, Y. Preparation and characterization of bioactive monolayer and functionally graded coatings. *J. Mater. Sci. Mater. Med.* **1999**, *10*, 269–273. [CrossRef] [PubMed]
311. Heimann, R.B. Thermal spraying of biomaterials. *Surf. Coat. Technol.* **2006**, *201*, 2012–2019. [CrossRef]
312. Goller, G. The effect of bond coat on mechanical properties of plasma sprayed bioglass-titanium coatings. *Ceram. Int.* **2004**, *30*, 351–355.
313. Oktar, F.N.; Yetmez, M.; Agathopoulos, S.; Loper Goerne, T.M.; Goller, G.; Ipeker, I.; Ferreira, J.M.F. Bond-coating in plasma-sprayed calcium-phosphate coatings. *J. Mater. Sci. Mater. Med.* **2006**, *17*, 1161–1171. [CrossRef]

314. Yang, Y.Z.; Tian, J.M.; Tian, J.T.; Chen, Z.Q.; Deng, X.J.; Zhang, D.H. Preparation of graded porous titanium coatings on titanium implant materials by plasma spraying. *J. Biomed. Mater. Res.* **2000**, *52*, 333–337. [CrossRef]
315. Ning, C.Y.; Wang, Y.J.; Chen, X.F.; Zhao, N.R.; Ye, J.D.; Wu, G. Mechanical performances and microstructural characteristics of plasma-sprayed bio-functionally gradient HA-ZrO_2-Ti coatings. *Surf. Coat. Technol.* **2005**, *200*, 2403–2408. [CrossRef]
316. Sun, J.; Thian, E.S.; Fuh, J.Y.H.; Chang, L.; Hong, G.S.; Wang, W.; Tay, B.Y.; Wong, Y.S. Fabrication of bio-inspired composite coatings for titanium implants using the micro-dispensing technique. *Microsyst. Technol.* **2012**, *18*, 2041–2051. [CrossRef]
317. Sola, A.; Bellucci, D.; Cannillo, V. Functionally graded materials for orthopedic applications—An update on design and manufacturing. *Biotechnol. Adv.* **2016**, *34*, 504–531. [CrossRef] [PubMed]
318. Schneider, K.; Heimann, R.B.; Berger, G. Plasma-sprayed coatings in thesystem CaO-TiO_2-ZrO_2-P_2O_5 for long-term stable endoprostheses. *Mater. Sci. Eng. Technol.* **2001**, *32*, 166–171.
319. Levingstone, T.J.; Barron, N.; Ardhaoui, M.; Benyounis, K.; Looney, L.; Stokes, J. Application of response surface methodology in the design of functionally graded plasma sprayed hydroxyapatite coatings. *Surf. Coat. Technol.* **2017**, *313*, 307–318. [CrossRef]
320. Chen, C.C.; Huang, T.H.; Kao, C.T.; Ding, S.J. Characterization of functionally graded hydroxyapatite/titanium composite coatings plasma sprayed on Ti alloys. *J. Biomed. Mater. Res. Part B Appl. Biomater.* **2006**, *78B*, 146–152. [CrossRef]
321. Cannillo, V.; Lusvarghi, L.; Sola, A. Design of Experiments (DOE) for the optimization of titania-hydoxyapatite functionally graded coatings. *Int. J. Appl. Ceram. Technol.* **2009**, *6*, 537–550. [CrossRef]
322. Tan, Y.; Wang, X.; Wu, Q.; Yan, W. Early peri-implant osteogenesis with functionally graded nanophase hydroxyapatite/bioglass coating on Ti alloys. *Key Eng. Mater.* **2007**, *330–332*, 553–556. [CrossRef]
323. Chen, X.; Zhang, B.; Gong, Y.; Zhou, P.; Li, H. Mechanical properties of nanodiamond-reinforced hydroxyapatite composite coatings deposited by suspension plasma spraying. *Appl. Surf. Sci.* **2018**, *439*, 60–65. [CrossRef]
324. Li, Z.; Khun, N.W.; Tang, X.Z.; Liu, E.; Khor, K.A. Mechanical, tribological and biological properties of novel 45S5 Bioglass composites reinforced with in situ reduced graphene oxide. *J. Mech. Behav. Biomed. Mater.* **2017**, *65*, 77–89. [CrossRef]
325. Zhang, C.; Xu, H.; Geng, X.; Wang, J.; Xiao, J.; Zhu, P. Effect of spray distance on microstructure and tribological performance of suspension plasma-sprayed hydroxyapatite–titania composite coatings. *J. Therm. Spray Technol.* **2016**, *25*, 1255–1263. [CrossRef]
326. Jaworski, R.; Pawłowski, L.; Pierlot, C.; Roudet, F.; Kozerski, S.; Petit, F. Recent developments in suspension plasma sprayed titanium oxide and hydroxyapatite coatings. *J. Therm. Spray Technol.* **2010**, *19*, 240–247. [CrossRef]
327. Fujishima, A.; Honda, K. Electrochemical photolysis of water at a semiconductor electrode. *Nature* **1972**, *238*, 37–38. [CrossRef] [PubMed]
328. Herrmann, J.-M.; Guillard, C. Photocatalytic degradation of pesticides in agriculturals used waters. *C.R. Acad. Sci.* **2000**, *3*, 417–422. [CrossRef]
329. Fujishima, A.; Rao, T.N.; Tryk, D.A. Titanium dioxide photocatalysis. *J. Photochem. Photobiol. C* **2000**, *1*, 1–21. [CrossRef]
330. Mills, A.; Le Hunte, S. An overview of semiconductor photocatalysis. *J. Photochem. Photobiol. A* **1997**, *108*, 1–35. [CrossRef]
331. Fujishima, A.; Zhang, X.; Tryk, D.A. TiO_2 photocatalysis and related surface phenomena. *Surf. Sci. Rep.* **2008**, *63*, 515–582. [CrossRef]
332. Ye, F.; Ohmori, A. The photocatalytic activity and photo-absorption of plasma sprayed. *Surf. Coat. Technol.* **2002**, *160*, 62–67. [CrossRef]
333. Ye, F.; Tsumura, T.; Nakata, K.; Ohmori, A. Dependence of photocatalytic activity on the compositions and photo-absorption of functional TiO_2-Fe_3O_4 coatings deposited by plasma spray. *Mater. Sci. Eng. B* **2008**, *148*, 154–161. [CrossRef]
334. Yu, Q.; Zhou, C.; Wang, X. Influence of plasma spraying parameter on microstructure and photocatalytic properties of nanostructured TiO_2-Fe_3O_4 coating. *J. Mol. Catal. A Chem.* **2008**, *283*, 23–28. [CrossRef]
335. Chen, H.; Lee, S.W.; Kim, T.H.; Hur, B.Y. Photocatalytic decomposition of benzene with plasma sprayed TiO_2-based coatings on foamed aluminum. *J. Eur. Ceram. Soc.* **2006**, *26*, 2231–2239. [CrossRef]
336. Ctibor, P.; Pala, Z.; Stengl, V.; Musalek, R. Photocatalytic activity of visible-light-active iron-doped coatings prepared by plasma spraying. *Ceram. Int.* **2014**, *40*, 2365–2372. [CrossRef]
337. Zenh, Y.; Liu, J.; Wu, W.; Ding, C. Photocatalytic performance of plasma sprayed $TiO_2ZnFe_2O_4$ coatings. *Surf. Coat. Technol.* **2005**, *200*, 2398–2402.

338. Daram, P.; Banjongprasert, C.; Thongsuwan, W.; Jiansirisomboon, S. Microstructure and photocatalytic activities of thermal sprayed titanium dioxide/carbon nanotubes composite coatings. *Surf. Coat. Technol.* **2016**, *306*, 290–294. [CrossRef]
339. Robotti, M.; Dosta, S.; Fernandez-Rodriguez, C.; Hernandez-Rodriguez, M.J.; Cano, I.G.; Pulido Melian, E.; Guilemany, J.M. Photocatalytic abatement of NOx by C-TiO_2/polymer composite coatings obtained by low pressure cold gas spraying. *Appl. Surf. Sci.* **2016**, *362*, 274–280. [CrossRef]
340. Liu, Y.; Huang, J.; Ding, S.; Liu, Y.; Yuan, J.; Li, H. Deposition, characterization and enhanced adherence of *Escherichia coli* bacteria on flame-sprayed photocatalytic titania-hydroxyapatite coatings. *J. Therm. Spray Technol.* **2013**, *22*, 1053–1062. [CrossRef]
341. Huang, J.; Gong, Y.; Liu, Y.; Suo, X.; Li, H. Developing titania-hydroxyapatite-reduced graphene oxide nanocomposite coatings by liquid flame spray deposition for photocatalytic applications. *J. Eur. Ceram. Soc.* **2017**, *37*, 3705–3711. [CrossRef]
342. Pawłowski, L. Technology of thermally sprayed anilox rolls: State of art, problems, and perspectives. *J. Therm. Spray Technol.* **1996**, *5*, 317–334. [CrossRef]
343. Kozerski, S.; Białucki, P.; Kaczmarek, M.; Ambroziak, A. Properties of Weld Overlays on Regenerated Wheel Hub of a Mining Vehicle. Ph.D. Thesis, Wrocław University of Science and Technology, Wrocław, Poland. Unpublished data.
344. Oerlikon Metco. TriplexPro-210 Plasma Spay Gun. Available online: https://www.oerlikon.com/metco/en/products-services/coating-equipment/thermal-spray/spray-guns/coating-equipment-plasma/triplexpro-210/ (accessed on 20 June 2020).
345. Tomaszek, R.; Pawłowski, L.; Zdanowski, J.; Grimblot, J.; Laurens, J. Microstructural transformations of TiO_2, Al_2O_3 + 13TiO_2 and Al_2O_3 + 40TiO_2 at plasma spraying and laser engraving. *Surf. Coat. Technol.* **2004**, *185*, 137–149. [CrossRef]
346. Kiilakoski, J.; Trache, R.; Bjorklund, S.; Joshi, S.; Vuoristo, P. Process parameter impact on suspension-HVOF-sprayed Cr_2O_3 coatings. *J. Therm. Spray Technol.* **2019**, *28*, 1933–1944. [CrossRef]
347. Pawłowski, L. Strategic oxides for thermal spraying: Problems of availability and evolution of prices. *Surf. Coat. Technol.* **2013**, *220*, 14–19. [CrossRef]
348. Tanaka, M.; Takatani, Y. Evaluation of sealants on Al–Zn alloy sprayed coating by galvanostatic technique. In *Thermal Spray 2001: New Surfaces for a New Millenium*; Berndt, C.C., Khor, K.A., Lugscheider, E.F., Eds.; ASM International: Materials Parks, OH, USA, 2001; pp. 621–625.
349. Praxair Surface Technologies. Get the Best Possible Treatment. Available online: https://www.praxairsurfacetechnologies.com/en/solutions-for-your-industry/printing-and-converting/corona-treating (accessed on 20 June 2020).
350. Feng, Y.; Li, Y.; Luo, Z.; Ling, Z.; Wang, Z. Resistance spot welding of Mg to electro-galvanized steel with hot-dip galvanized steel interlayer. *J. Mater. Process. Technol.* **2016**, *236*, 114–122. [CrossRef]
351. Patel, V.K.; Bhole, S.D.; Chen, D.L. Characterization of ultrasonic spot-welded joints of Mg-to-galvanized and ungalvanized steel with a tin interlayer. *J. Mater. Process. Technol.* **2014**, *214*, 811–817. [CrossRef]
352. Gu, X.; Sui, C.; Liu, J.; Li, D.; Meng, Z.; Zhu, K. Microstructure and mechanical properties of Mg/Al joints welded byultrasonic spot welding with Zn interlayer. *Mater. Des.* **2019**, *181*, 108103. [CrossRef]
353. Winnicki, M.; Małachowska, A.; Korzeniowski, M.; Jasiorski, M.; Baszczuk, A. Aluminium to steel resistance spot welding with cold sprayed interlayer. *Surf. Eng.* **2017**, *34*, 235–242. [CrossRef]
354. Wojdat, T.; Winnicki, M.; Rutkowska-Gorczyca, M.; Krupiński, S.; Kubica, K. Soldering aluminium to copper with the use of interlayers deposited by cold spraying. *Arch. Civ. Mech. Eng.* **2016**, *16*, 835–844. [CrossRef]
355. Li, J.F.; Agyakwa, P.A.; Johnson, C.M.; Zhang, D.; Hussain, T.; McCartney, D.G. Characterization and solderability of cold sprayed Sn–Cu coatings on Al and Cu substrates. *Surf. Coat. Technol.* **2010**, *204*, 1395–1404. [CrossRef]
356. Wojdat, T.; Winnicki, M.; Łamasz, S.; Żuk, A. Application of interlayers in the soldering process of graphite composite to aluminium alloy 6060. *Arch. Civ. Mech. Eng.* **2019**, *19*, 91–99. [CrossRef]
357. Yang, K.; Li, W.; Huang, C.; Yang, X.; Xu, Y. Optimization of cold-sprayed AA2024/Al_2O_3 metal matrix composites via friction stir processing: Effect of rotation speeds. *J. Mater. Sci. Technol.* **2018**, *34*, 2167–2177. [CrossRef]
358. Peat, T.; Galloway, A.; Toumpis, A.; McNutt, P.; Iqbal, N. The erosion performance of cold spray deposited metal matrix composite coatings with subsequent friction stir processing. *Appl. Surf. Sci.* **2017**, *396*, 1635–1648. [CrossRef]

359. Huang, C.; Li, W.; Zhang, Z.; Fu, M.; Planche, M.P.; Liao, H.; Montavon, G. Modification of a cold sprayed SiC p/Al5056 composite coating by friction stir processing. *Surf. Coat. Technol.* **2016**, *296*, 69–75. [CrossRef]
360. Hodder, K.J.; Izadi, H.; McDonald, A.G.; Gerlich, A.P. Fabrication of aluminum–alumina metal matrix composites via cold gas dynamic spraying at low pressure followed by friction stir processing. *Mater. Sci. Eng. A* **2012**, *556*, 114–121. [CrossRef]
361. Peat, T.; Galloway, A.; Toumpis, A.; Steel, R.; Zhu, W.; Iqbal, N. Enhanced erosion performance of cold spray co-deposited AISI316 MMCs modified by friction stir processing. *Mater. Des.* **2017**, *120*, 22–35. [CrossRef]
362. Yang, K.; Li, W.; Xu, Y.; Yang, X. Using friction stir processing to augment corrosion resistance of cold sprayed AA2024/Al_2O_3 composite coatings. *J. Alloys Compd.* **2019**, *774*, 1223–1232. [CrossRef]
363. Gupta, N.; Doddamani, M. Polymer matrix composites. *J. Met.* **2018**, *70*, 1282–1283. [CrossRef]
364. Afshar, A.; Mihut, D.; Hill, S.; Baqersad, J. Synergistic effects of environmental exposures on polymer matrix with or without metallic coating protection. *J. Compos. Mater.* **2018**, *52*, 3773–3784. [CrossRef]
365. Che, H.; Chu, X.; Vo, P.; Yue, S. Metallization of various polymers by cold spray. *J. Therm. Spray Technol.* **2018**, *27*, 169–178. [CrossRef]
366. Khalkhali, Z.; Rothstein, J.P. Characterization of the cold spray deposition of a wide variety of polymeric powders. *Surf. Coat. Technol.* **2020**, *383*, 125251. [CrossRef]
367. Małachowska, A.; Winnicki, M.; Konat, Ł.; Piwowarczyk, T.; Pawłowski, L.; Ambroziak, A.; Stachowicz, M. Possibility of spraying of copper coatings on polyamide 6 with low pressure cold spray method. *Surf. Coat. Technol.* **2017**, *318*, 82–89. [CrossRef]
368. Yang, S.-Y.; Ji, M. Polyimide matrices for carbon fiber composites. In *Advanced Polyimide Materials*; Yang, S.-Y., Ed.; Elsevier: Amsterdam, The Netherlands, 2018; pp. 93–136.
369. Huang, W.; Zhao, Y.; Fan, X.; Meng, X.; Wang, Y.; Cai, X.; Cao, X.; Wang, Z. Effect of bond coats on thermal shock resistance of thermal barrier coatings deposited onto polymer matrix composites via air plasma spray process. *J. Therm. Spray Technol.* **2013**, *22*, 918–925. [CrossRef]
370. Huang, W.; Gan, X.; Zhu, L. Fabrication and property of novel double-layer coating deposited on polyimide matrix composites by atmospheric plasma spraying. *Ceram. Int.* **2018**, *44*, 5473–5485. [CrossRef]
371. Zhu, L.; Huang, W.; Cheng, H.; Cao, X. Thermal shock resistance of stabilized zirconia/metal coat on polymer matrix composites by thermal spraying process. *J. Therm. Spray Technol.* **2014**, *23*, 1312–1322. [CrossRef]
372. Abedi, H.R.; Salehi, M.; Shafyei, A. Microstructure, tensile adhesion strength and thermal shock resistance of TBCs with different flame-sprayed bond coat materials onto BMI polyimide matrix composite. *J. Therm. Spray Technol.* **2017**, *26*, 1669–1684. [CrossRef]
373. Ivosevic, M.; Knight, R.; Kalidindi, S.R.; Palmese, G.R.; Sutter, J.K. Solid particle erosion resistance of thermally sprayed functionally graded coatings for polymer matrix composites. *Surf. Coat. Technol.* **2006**, *200*, 5145–5151. [CrossRef]
374. Ivosevic, M.; Gupta, V.; Baldoni, J.A.; Cairncross, R.A.; Twardowski, T.E.; Knight, R. Effect of substrate roughness on splatting behavior of HVOF sprayed polymer particles: Modeling and experiments. *J. Therm. Spray Technol.* **2006**, *15*, 725–730. [CrossRef]
375. Ivosevic, M.; Knight, R.; Kalidindi, S.R.; Palmese, G.R.; Sutter, J.K. Erosion/oxidation resistant coatings for high temperature polymer composites. *High Perform. Polym.* **2003**, *15*, 503–517. [CrossRef]
376. Liu, A.; Guo, M.; Zhao, M.; Ma, H.; Hu, S. Arc sprayed erosion-resistant coating for carbon fiber reinforced polymer matrix composite substrates. *Surf. Coat. Technol.* **2006**, *200*, 3073–3077. [CrossRef]
377. Cui, Y.; Guo, M.; Wang, C.; Tang, Z. Adhesion enhancement of a metallic al coating fabricated by detonation gun spray on a modified polymer matrix composite. *J. Therm. Spray Technol.* **2019**, *28*, 1730–1738. [CrossRef]
378. Rezzoug, A.; Abdi, S.; Kaci, A.; Yandouzi, M. Thermal spray metallisation of carbon fibre reinforced polymer composites: Effect of top surface modification on coating adhesion and mechanical properties. *Surf. Coat. Technol.* **2018**, *333*, 13–23. [CrossRef]
379. Chen, W.R.; Irissou, E.; Wu, X.; Legoux, J.G.; Marple, B.R. The oxidation behavior of TBC with cold spray CoNiCrAlY bond coat. *J. Therm. Spray Technol.* **2011**, *20*, 132–138. [CrossRef]
380. Karaoglanli, A.C.; Turk, A. Isothermal oxidation behavior and kinetics of thermal barrier coatings produced by cold gas dynamic spray technique. *Surf. Coat. Technol.* **2017**, *318*, 72–81. [CrossRef]
381. Khanna, A.S.; Rathod, W.S. Development of CoNiCrAlY oxidation resistant hard coatings using high velocity oxy fuel and cold spray techniques. *Int. J. Refract. Hard Met.* **2015**, *49*, 374–382. [CrossRef]

382. Go, T.; Sohn, Y.J.; Mauer, G.; Vassen, R.; Gonzalez-Julian, J. Cold spray deposition of Cr2AlC MAX phase for coatings and bond-coat layers. *J. Eur. Ceram. Soc.* **2019**, *39*, 860–867. [CrossRef]
383. Gardon, M.; Melero, H.; Garcia-Giralt, N.; Dosta, S.; Cano, I.G.; Guilemany, J.M. Enhancing the bioactivity of polymeric implants by means of cold gas spray coatings. *J. Biomed. Mater. Res. Part B* **2014**, *102B*, 1537–1543. [CrossRef]
384. Arcos, D.; Vallet-Regi, M. Substituted hydroxyapatite coatings of bone implants. *J. Mater. Chem. B* **2020**, *8*, 1781–1800. [CrossRef] [PubMed]
385. Ullah, I.; Siddiqui, M.A.; Liu, H.; Kolawole, S.K.; Zhang, J.; Zhang, S.; Ren, L.; Yang, K. Mechanical, biological, and antibacterial characteristics of plasma-sprayed (Sr, Zn) substituted hydroxyapatite coating. *ACS Biomater. Sci. Eng.* **2020**, *6*, 1355–1366. [CrossRef]
386. Lyasnikova, A.V.; Markelova, O.A.; Dudareva, O.A.; Lyasnikov, V.N.; Barabash, A.P.; Shpinyak, S.P. Comprehensive characterization of plasma-sprayed coatings-based silver- and cooper-substituted hydroxyapatite, Powder Metall. *Met. Ceram.* **2016**, *55*, 328–333.
387. Unabia, R.B.; Bonebeau, S.; Candidato, R.T., Jr.; Pawłowski, L. Preliminary study on copper-doped hydroxyapatite coatings obtained using solution precursor plasma spray process. *Surf. Coat. Technol.* **2018**, *353*, 370–377. [CrossRef]
388. Bose, S.; Vu, A.A.; Emshadi, K.; Bandyopadhyay, A. Effects of polycaprolactone on alendronate drug release from Mg-doped hydroxyapatite coating on titanium. *Mater. Sci. Eng. C* **2018**, *88*, 166–171. [CrossRef]
389. Cao, L.; Ullah, I.; Li, N.; Niu, S.; Sun, R.; Xia, D.; Yang, R.; Zhang, X. Plasma spray of biofunctional (Mg, Sr)-substituted hydroxyapatite coatings for titanium alloy implants. *J. Mater. Sci. Technol.* **2019**, *35*, 719–726. [CrossRef]
390. Chen, Y.; Zheng, X.; Xie, Y.; Ding, C.; Ruan, H.; Fan, C. Anti-bacterial and cytotoxic properties of plasma sprayed silver-containing HA coatings. *J. Mater. Sci. Mater. Med.* **2008**, *19*, 3603–3609. [CrossRef]
391. Chen, Y.; Zheng, X.; Xie, Y.; Ji, H.; Ding, C.; Li, H.; Dai, K. Silver release from silver-containing hydroxyapatite coatings. *Surf. Coat. Technol.* **2010**, *205*, 1892–1896. [CrossRef]
392. Shimazaki, T.; Miyamoto, H.; Ando, Y.; Noda, I.; Yonekura, Y.; Kawano, S.; Miyazaki, M.; Mawatari, M.; Hotokebuchi, T. In vivo antibacterial and silver-releasing properties of novel thermal sprayed silver-containing hydroxyapatite coating. *J. Biomed. Mater. Res. B* **2010**, *92*, 386–389.
393. Fielding, G.A.; Roy, M.; Bandyopadhyay, A.; Bose, S. Antibacterial and biological characteristics of silver containing and strontium doped plasma sprayed hydroxyapatite coatings. *Acta Biomater.* **2012**, *8*, 3144–3152. [CrossRef]
394. Cizek, J.; Brozek, V.; Chraska, T.; Lukac, F.; Medricky, J.; Musalek, R.; Tesar, T.; Siska, F.; Antos, Z.; Cupera, J.; et al. Silver-doped hydroxyapatite coatings deposited by suspension plasma spraying. *J. Therm. Spray Technol.* **2018**, *27*, 1333–1343. [CrossRef]
395. Singh, B.; Singh, G.; Sidhu, B.S.; Bhatia, N. In-vitro assessment of HA-Nb coating on Mg alloy ZK60 for biomedical applications. *Mater. Chem. Phys.* **2019**, *231*, 138–149. [CrossRef]
396. Heimann, R.B.; Kleiman, J.I.; Litovsky, E.; Marx, S.N.R.; Petrov, S.; Shagalov, M.; Sodhi, R.N.S.; Tang, A. High-pressure cold gas dynamic (CGD)-sprayed alumina-reinforced aluminum coatings for potential application as space construction material. *Surf. Coat. Technol.* **2014**, *252*, 113–119. [CrossRef]